Damping of machine tool structures with riveted joints

A THESIS SUBMITTED IN PARTIAL FULFILLMENT

OF THE REQUIREMENTS FOR THE DEGREE OF

MASTER OF TECHNOLOGY

IN

MECHANICAL ENGINEERING

BY

Pavan Kumar Vodnala

209ME2211

DEPARTMENT OF MECHANICAL ENGINEERING

NATIONAL INSTITUTE OF TECHNOLOGY

ROURKELA

2011

Damping of machine tool structures with riveted joints

A THESIS SUBMITTED IN PARTIAL FULFILLMENT

OF THE REQUIREMENTS FOR THE DEGREE OF

MASTER OF TECHNOLOGY

IN

MECHANICAL ENGINEERING

BY

Pavan Kumar Vodnala

209ME2211

UNDER THE GUIDANCE OF

Prof. B.K. NANDA

DEPARTMENT OF MECHANICAL ENGINEERING

NATIONAL INSTITUTE OF TECHNOLOGY

ROURKELA

2011

National Institute of Technology

Rourkela

CERTIFICATE

This is to certify that the thesis entitled, **"DAMPING OF MACHINE TOOL STRUCTURES WITH RIVETED JOINTS"** submitted by Mr. Pavan Kumar Vodnala in partial fulfillment of the requirements for the award of *Master of Technology* degree in *Mechanical Engineering* with specialization in *Production Engineering* during session 2009-2011 at the National Institute of Technology, Rourkela (Deemed University) is an authentic work carried out by him under my supervision and guidance. To the best of my knowledge, the matter embodied in the thesis has not submitted to any other University/Institute for the award of any degree or diploma.

Date:

Prof. B.K. Nanda

Dept. of Mechanical Engg.

National Institute of Technology

Rourkela

ACKNOWLEDGEMENT

I express my deep sense of gratitude and reverence to my thesis supervisor **Prof. B. K. Nanda**, Professor, Mechanical Engineering Department, National Institute of Technology, Rourkela, for his invaluable encouragement, helpful suggestions and supervision throughout the course of this work and providing valuable department facilities.

I would like to thank **Prof. R.K. Sahoo**, Head of the Department, **Prof. S. S. Mahapatra,** PG coordinator of the Mechanical Engineering Department and **Prof. K. P. Maity**, faculty Adviser.

I would like to thank technicians of Dynamics lab, for their timely help in conducting the experiment.

Last but not least I would like to thank **Mr. Bhagat Singh** (Ph.D. scholar) and well-wishers who are involved directly or indirectly in successful completion of the present work.

Date **(Pavan Kumar vodanala)**

209ME2211

Nomenclature

English Symbols

A	Area of cross-section of the beam
A_o	Area of cross-section of the rivet
A'	Area under a connecting rivet head
d	Diameter of connecting rivet
E	Static bending modulus of elasticity
E_f	Energy loss per cycle due to friction at joints
E_{loss}	Total energy loss per cycle
E_n	Energy stored in the system per cycle
E_o	Energy loss per cycle due to material and support friction
F_{rM}	Maximum frictional force at the interfaces
$2h_1$, $2h_2$	Thickness of each layer of the cantilever specimen
I	Second moment of area
k	Static bending stiffness of the layered and jointed beam
k'	Static bending stiffness of the solid beam
l	Length of individual elements
L	Free length of the layered and jointed beam
m	Number of layers in a jointed beam
N	Total normal force under each connecting rivet
p	Interface pressure

P	Preload on a rivet
q	Number of rivets
R	Any radius within influencing zone
R_B	Radius of the connecting rivet
R_M	Limiting radius of influencing zone
t	time coordinate
u_o	Relative dynamic slip between the interfaces at a riveted joint in the absence of friction
u_r	Relative dynamic slip between the interfaces at a riveted joint in the presence of friction
u_{rM}	Relative dynamic slip between the interfaces at the maximum amplitude of vibration
W	Static load
a_1, a_{n+1}	Amplitude of first cycle and last cycle, respectively
$y(l, 0)$	Initial free end displacement
n	Number of cycles

Greek Symbols

α	Dynamic slip ratio $\left(u_r/u_o\right)$
δ	Logarithmic decrement of the system
Δ	Deflection due to static load
μ	Kinematic coefficient of friction
ω_n	Natural frequency of vibration
ω_d	Damped frequency of vibration
ρ	Mass density

σ_o	Initial stress on a rivet
σ_S	Surface stress on the jointed structure
ξ	Damping ratio

Operators

‘.’	$\frac{d}{dt}$
‘,’	$\frac{d}{dx}$

CONTENTS

LIST OF FIGURES:

LIST OF TABLES:

Abstract:

Light weight structures typically have low inherent structural damping. The damping mechanism of jointed and riveted structures can be explained by considering the energy loss due to friction and the dynamic slip produced at the interfaces. The frictional damping is evaluated from the relative slip between the jointed interfaces and is considered to be the most useful method for investigating the structural damping. The damping characteristics in jointed structures are influenced by the intensity of pressure distribution, micro-slip and kinematic coefficient of friction at the interfaces and the effects of all these parameters on the mechanism of damping have been extensively studied. All the above vital parameters are largely influenced by the thickness ratio of the beam and thereby affect the damping capacity of the structures. In addition to this, number of layers, beam length and diameter of connecting rivet also play key roles on the damping capacity of the jointed structures quantitatively. The effects of all these parameters are studied vividly in the present investigation. It is established that the damping capacity can be enhanced appreciably using larger beam length and rivet diameters as well as lower thickness ratio of the beams. Further improvement in damping is possible with the use of more number of layers compared to its equivalent solid one. This design concept of using layered structures with riveted joints can be effectively utilized in trusses and frames, aircraft and aerospace structures, bridges, machine members, robots and many other applications where higher damping is required. Extensive experiments have been conducted on a number of mild steel specimens under different initial conditions of excitation for establishing the authenticity of the theory developed.

CHAPTER – 1

INTRODUCTION

1. INTRODUCTION:

With rapid growth and development of sophisticated structures, efforts have been made by engineers and technologists to improve their damping capabilities by controlling disastrous effects of vibrations through foundations and proper design of structures. The study of dynamics of fabricated structures enables the engineers to design machines tools to minimize the machining errors that are likely to occur under dynamic condition, viz. deflection error, positional error, error due to vibrational instability, etc. The continuous trend towards lighter structures, low noise, increased reliability, highly balance, less vibration transmission to foundation and long life at higher operating speed requires that abundant research scope still exists in this field. In real engineering fields, damping is a heterogeneous mix of various types of damping mechanisms ranging from coulomb type to the type where the damping force varies as the nth power of velocity. It is this complex combination of damping mechanism which makes the analytical study of damping complicated. Hence, damping studies are mainly experimental in nature and all problems of damping are to be ultimately resolved through experimental analysis. With the development of jointed beams, the fabricated structures can be used as a replacement for solid structures with enhanced damping.

1.1. DAMPING:

Term damping refers to the energy dissipation properties of a material or a system under cyclic stress but excludes energy transfer device. When a structure is subjected to an excitation by an external force then it vibrates in certain amplitude of vibration, it reduces as the external

force is removed. This is due to some resistance offered to the structural member which may be internal or external. This resistance is termed as damping.

1.1.1. CLASSIFICATION OF DAMPING:

Damping can be broadly divided into two classes depending on their sources,

(1) Material damping

(2) System damping

MATERIAL DAMPING:

Damping due to dissipative mechanism working inside the material of the member is termed as material damping. The magnitude of material damping in structural metal is low and depends upon the level of stressing. Actual value of stress level for a definite resonant frequency however depends upon the deflection of structural member. Material with best fatigue strength is not necessarily the best material for near resonant loading. Ferro-magnetic material and alloys of magnesium and cobalt exhibits higher damping than common structural material, iron, steel, or aluminum.

SYSTEM DAMPING:

System damping involves configuration of distinguishable part arises from slip and boundary shear effects of mating surfaces. Energy dissipation during cyclic stress at an interface

may occur as a result of dry sliding (coulomb friction), lubricated sliding (viscous forces) or cyclic strain in a separating adhesive (damping in visco-elastic layers between mating surfaces). System damping to our need is classified as:

(1) Support damping

(2) Damping due to sandwich construction

(3) Damping due to joints

CLASSIFICATION OF JOINTS ACCORDING TO CONFIGURATION:

An important step towards the analysis and representation of the mode of vibration of machine is the analysis of spatial vibration behavior of the structure when vibrating in its resonance frequencies. In order to examine a machine from structural point of view it is necessary to provide a method by which a structural mode is abstracted from a machine. The modular construction system for machine tool has recently become important not only to rationalize their design and manufacturing procedure but also to evolve a feasible manufacturing system. Fundamental shape, main cross-sectional shape and function of structural modules and relation between adjacent structural configuration shows that a machine consists of many elementary aggregate. This hierarchical property of machine structure suggests the possibility of defining a concrete model suitable for each joint in machine tool. Following fundamental characteristics of the joint are to be considered when replacing machine tool joints by mathematical model:

(1) The static stiffness of structures with joints is considerably lower than that of the equivalent solid structures and joint stiffness show the non-linear characteristics.

(2) The damping capacity of jointed structures is higher than that of equivalent solid one, but the natural frequency of jointed structures is less as compared to solid one.

(3) The characteristics mentioned above are in large dependence on the stiffness ratio of joint surrounding.

Sliding joint:

Here joint displacement to sum of the roughness ratio is smaller than unity. The ratio also increases with an increasing interface pressure. In plain slide-ways the dynamic characteristics are mainly determined by damping caused by friction, the mass of the carriage and the stiffness and damping of the drive. The stiffness and the damping of the practical fabricated structures are not always linear because of the existence of a certain preload is considered. The damping caused by friction is non-linear and may be either positive or negative which means either stable sliding or self-excited oscillations (stick-slip). Measurement shows that damping depends upon slide ways materials, velocity, lubricant and mass. Mechanism of damping in a joint is not merely due to friction but is a complex one of micro and macro friction and cyclic plastic deformation is likely to be predominant mechanism to which energy dissipation could be attributed.

(1) Macro-slip involving frictional damping

(2) Micro-slip involving very small displacement of asperities with respect to other surface.

1.1.2. DAMPING DUE TO SANDWICH CONSTRUCTION:-

The forced vibration of beams and plates can be reduced by inserting a layer of damping material at attachment point and by permitting some motion to take place. Core thickness equal to or greater than the thickness of the metal constraining layer can provide high overall damping. Artificial means of effecting interfacial damping is envisaged namely bolted, riveted, welded, laminated adhesive joint to serve the dual purpose of fasting and damping the vibration. Structural member can be joined by adhesive, fastener and welding method.

DIFFERENT TECHNIQUES OF DAMPING

(i) Unconstrained construction:

Layer of viscoelastic layer is bonded to elastic one. In this case the viscoelastic layer to elastic one, the viscoelastic layer is subjected to alternate extension and compression as the elastic layer to which it is bonded experiences flexural vibrations, mostly applied to finished material structure like automobile bodies, ship hulls, and air craft skin.

(ii) Constrained construction:

Viscoelastic layer is sandwiched between two elastic layers. Such an arrangement vibrating in bending would cause shear strain in viscoelastic layer, causing energy dissipation. This type used in printed circuit board for air craft missiles, mounting platforms for electronic and guidance apparatus, air craft and missile structure, building bridges, ship engine. Constrained

type of treatment is seen to be more beneficial in practice as it is seen to be more beneficial in practice as it is seen to provide more damping for the same total weight of structure. Adhesive layer in the joint forms an equivalent solid coupling. Cyclic damping produced in thin layers of dissipative material placed between two rigid surfaces is inversely proportional to adhesive layer thickness.

(iii)Laminated construction:

Damping in plate type of structure can be significantly increased by using laminated plates correctly fastened to allow interfacial slip during vibration. We know that considerable damping can be achieved by using viscoelastic material in structures; the damping capacity of material is both frequency and temperature sensitive to a much greater extent than that found in friction, so that their use in the condition of changing temperature and frequency is limited. Viscoelastic material is an extra structural element, so that further advantage of frictional damping is that it does not require extra space for damping material to be filled in the structure. In this case panel of thickness t is replaced by n laminates of total thickness T (each of thickness T/n). The laminates were fastened together in such a way that as the panel vibrates interfacial slip occurs between laminates, thus giving rise to frictional damping. This can be achieved by riveting. Some suggestions are given for interface preparation and its effects on frictional damping in joint. If fretting occurs in a joint at least two undesirable effects may occur.

(i) Fretting may introduce serious corrosion damage within the joint and initiate crack with ultimate fatigue failure.

(ii) The fretting action may allow the joint to drift from any present clamping condition or even cause jamming at critical clearance.

Shot peening and blasting both increase surface roughness and reduce surface damage compared with ground surface, while metal spray show little surface damage but introduce some instability in joint. However cyanide hardened surface show very stable condition with slight surface damage without impairing energy dissipation capability of joint. As the material damping within the structural members is of low magnitude, various other techniques are used to improve the damping capacity of structures. These are: (i) Use of constrained/unconstrained viscoelastic layers, (ii) fabrication using a multi-layered sandwich construction, (iii) use of stress raisers, (iv) insertion of special high-elasticity inserts in the parent structure, (v) application of spaced damping techniques, (vi) use of a viscous fluid layer, (vii) use of bonded joints and (viii) fabricating layered and jointed structures with riveted joints.

1.1.3. DAMPING CAPACITY OF RIVETED JOINT:-

Damping capacity of a riveted joint depends mainly on the following factors:

(i) Co-efficient of friction between joint surfaces.

(ii) Micro-slip between joint surfaces

(iii) Reaction force of a base applied during vibration

(iv)Joint material, machining method of joint surfaces, interfacial layers, thickness of the beam, amplitude of vibration has large effect on damping and frequency.

1.1.4. DAMPING RATIO OF BEAM:

Recently demand for machine tools and fabricated structures having a high stiffness is increasing and it is widely recognized that the machine tools and fabricated structures should have a high static stiffness together with a light weight. For this purpose the riveted steel construction is very suitable, and then the use of machine tools made of riveted structures has been examined frequently up to the present. Many studies have been made on the sandwiched beam, the jointed beam and the laminated beam, and some of these beams have been already used practically.

1.2 OBJECTIVE:

Built-up structures are generally fabricated using many types of fasteners such as bolted, riveted and welded joints. It is the well-known fact that the improvement in damping due to the provision of welded joints is not appreciable compared to the use of bolted or riveted joints. Therefore, the use of welded joints is usually avoided in structural applications where higher damping is the main criterion. In case of bolted and riveted joints, the fundamental mechanism of damping may be same, but they differ in their functional aspects. For example, the parameters such as interface pressure distribution characteristics, zone of influence and preload are not same in both cases. Since the zone of influence differs in both cases, the relative spacing among the joints will be different thereby changing the relative dynamic slip at the interfaces. These facts suggest that the damping action for both cases is not same. Further, the axial load on a bolt can be varied by applying the tightening torque as per the clamping requirements of the structure whereas the preload in a rivet is constant and cannot be changed in the latter part of the design.

Although, a lot of analytical, computational and experimental works have been carried out by several researchers in the recent past on the damping of bolted structures, but no substantial work has been reported till date on the damping capacity of riveted structures. In this work a novel attempt has been made to study, both theoretically and experimentally, the damping in riveted joint construction and to compare their relative magnitudes. Consequently, it is highly desirable that the machine members, building structures and industries can definitely make use of jointed construction for the improvement of damping without sacrificing strength where vibration is encountered.

CHAPTER-2

LITERATURE SURVEY

2. LITERATURE SURVEY

Riveting is widely used for construction of many structures. Although a considerable amount of work has been reported on the study of damping in riveted structures with non-uniform pressure distribution at the interfaces, no generalized theory has been established for layered and riveted beams with uniform pressure distribution at the interfaces. Most engineering structures are built up by connecting structural components through mechanical connections. Such assembled structures need sufficient damping to limit excessive vibrations under dynamic loads. Damping in such structures mainly originates from two sources. One is the internal or material damping which is inherently low [1] and the other one is the structural damping due to joints [2]. The latter one offers an excellent source of energy dissipation, thereby adequately compensating the low material damping of structures. It is estimated that structures consisting of bolted or riveted members contribute about 90% of the damping through the joints [3]. The work in this thesis is oriented towards the use of mechanical systems fabricated in layers jointed with rivets for achieving increased damping.

As discussed in the preceding paragraph, the provision of layers in association with joints encourages large damping in built-up structures. These connections are recognized as a good source of energy dissipation and greatly affect the dynamic behavior in terms of natural frequency and damping [4, 5]. This structural damping offering excellent potential for large energy dissipation is associated with the interface shear of the joint. It is thus recognized that the provision of joints can effectively contribute to the damping of all fabricated structures. Although most of the inherent damping occurring in real structures arises in the joints, but a little effort has been made to study this source of damping because of complex mechanism occurring

at the interfaces due to relative slip, coefficient of friction and pressure distribution characteristics. It is therefore important to focus the attention to study these parameters for accurate assessment of the damping capacity of structures.

Over the past few decades, most of the work has been confined in the area of micro- and macro-slip phenomena [6, 7]. These concepts are utilized to study the dynamic behavior of jointed structures having friction contact [8-15]. This model is generally adopted when the normal load at the interface is small. On the other hand, many researchers [13, 14] have utilized the micro-slip concept considering the friction surface as an elastic body. In this case, the interface undergoes partial slip at high normal load. Masuko et al. [16] and Nishiwaki et al. [17, 18] have found out the energy loss in jointed cantilever beams considering micro-slip and normal force at the interfaces. Olofsson and Hagman [19] have shown that the micro-slip at the contacting surfaces occur when an optimum frictional load is applied. They have also presented a model for micro-slip between the flat smooth and rough surfaces covered with ellipsoidal elastic bodies.

The role of friction is of paramount importance in controlling the dynamic characteristics of engineering structures. This may be undesirable or desirable depending on the type of applications. Friction is often considered detrimental in the design of moving parts. On the other hand, this is desirable in fabricated structures for effective energy dissipation. Therefore, this concept of design is always considered in assembled structures requiring high damping. The friction at the jointed interfaces arises when the layers experience relative movement under transverse vibration. The Coulomb's law of friction is widely used to represent the dry friction at the contacting surfaces. The friction in a joint arises from shearing between the parts and is governed by the tension in the bolt/rivet, surface properties and type of materials in contact [20].

Den Hartog [21] has analytically solved the steady state response of a simple friction-damped system with combined Coulomb and viscous friction. Reviews on the effects of joint friction on structural damping in built-up structures have been presented by many researchers [22, 5, 23]. Their findings have shown that the friction in structural joints is regarded as a major source of energy dissipation in assembled structures.

The nature of pressure distribution across a beam layer is another important aspect affecting the damping capacity of jointed structures. Several workers have tried over the years to know the actual pattern of pressure distribution at the interfaces due to the clamping action on the joint. Almost all previous researchers have idealized the joints by assuming a uniform pressure profile without considering the effects of surface irregularities and asperities [16-18]. In fact, many authors [24-29] have conducted experiments to know the exact distribution characteristics. These experiments have confirmed that the interface pressure is hardly constant in actual situation. In particular, Gould and Mikic [28] and Ziada and Abd [29] have reported that the pressure distribution at the interfaces of a bolted joint is parabolic in nature circumscribing the bolt which is approximately 3.5 times the bolt diameter.

Recently, Nanda and Behera [30] have developed a theoretical ssssion for the pressure distribution at the interfaces of a bolted joint by curve fitting the earlier data reported by Ziada and Abd [31]. They have obtained an eighth order polynomial even function in terms of normalized radial distance from the centre of the bolt such that the function assumes its maximum value at the centre of the bolt and decreases radially away from the bolt. They have used Dunn's curve fitting software to calculate the exact spacing between bolts that would result in a uniform interfacial pressure distribution along the entire length of the beam. Using exact

spacing of 2.00211 times the diameter of the connecting bolts, Nanda and Behera have been successful in simulating uniform interface pressure over the length of the beam. Thereafter, they have investigated the effect of interface pressure on the behavior of interfacial slip damping.

Damisa et al. [32] have also recently carried out an analysis to study the effect of non-uniform pressure distribution on the mechanism of slip damping for layered beams, but their analysis is limited to static load. Later, they have extended their analysis to realistic dynamic loading for estimating the interfacial slip damping in clamped layered beams [34]. They have shown that under the action of dynamic loads, the factors like non-uniform pressure distribution as well as frequency variation have a significant effect on both the energy dissipation and logarithmic decrement associated with the mechanism of slip damping in layered structures. They have further reported that the amount of energy dissipation through slip damping under externally applied dynamic load is less than that of the corresponding static load. Olunloyo et al. [33] have used other forms of pressure distributions such as polynomial or hyperbolic representations but the results obtained have demonstrated that the effects of such distributions in comparison with the linear profile are largely incremental in nature.

There are various measuring methods available in practice to know the contact pressure between layers. The technique of using ultrasonic waves is most capable among them as it measures the real contact pressure without changing the characteristics of the contact surface. This measurement has produced fair results using a normal probe [36, 37]. However, the angle probe used by Minakuchi et al. [36] is more convenient to measure. They have found out the contact pressure between two layered beams of different thicknesses by establishing a relationship between the mean contact pressure and sound pressure of reflected waves. This method is widely

accepted as the experimental results fairly agree with the theoretical ones. The present investigation uses the numerical data of Minakuchi et al. [38] to obtain the theoretical equation for non-uniform pressure at the interfaces of a jointed beam by curve fitting with MATLAB software.

Energy dissipation resulting from slip and non-uniform pressure distribution in bolted joints has been the subject of many studies [28-30]. Some researchers [4, 39, 40] have reported different mechanisms of energy dissipation that might take place depending on the clamping pressure. Typically, the normal interfacial pressure across the clamped joint is not uniformly distributed. Under high pressure, the slip is small, while under low pressure the shear due to friction is small. An optimal clamping force exists somewhere between these two limits under which a joint dissipates maximum vibration energy. Beards [42] has looked into this aspect and recognized the existence of an optimum joint force for maximum energy dissipation. Jezequel [40] has proposed an algorithm for calculating the energy loss due to slip in bolted plates. It has been found that the joint friction exhibits viscous-like damping characteristics when the normal force is allowed to vary with the relative slip [43].

Beards and Williams [9] in their experimental investigation of a frame structure have shown that a useful increase in damping could be achieved by fastening joints tightly to prohibit translational slip, but not tightly enough to restrict rotational slip. Beards and Imam [8] have found that the frictional damping of plate-type structures is enhanced using fastened laminated plates having interfacial slip during vibration. In another study, Beards and Woodwat [42] have experimentally determined the effect of controlled frictional damping in joints on the frequency response of a frame under harmonic excitation.

In general, the introduction of riveted joints increases the amount of damping in addition to the inherent material damping of the equivalent monolithic construction. In the past, Pian and Hallowell [43] presented the theory of structural damping in built-up beams connected with riveted cover plates. Moreover, Pian [44] has carried out the theoretical analysis of energy dissipation of a continuously riveted spar and spar cap and found the results are in good agreement with the experimental ones. Further, Pian has established that the riveted joints are uniquely responsible for enhancing the damping levels in structures.

The above literature survey reveals that a great deal of work has been pursued in determining the damping capacity of bolted structures with little or no progress in the study of damping of riveted structures. In the context of the present investigation, a proper differentiation has to be made between the bolted and riveted connections in built-up structures in order to emphasize the present research. In both cases, the fundamental mechanism of damping is identical but they differ in their functional aspects. The parameters such as interface pressure distribution characteristics, zone of influence and preload are not the same. For example, the zone of interface pressure distribution circumscribing a rivet is equal to 4.125, 5.0 and 5.6 times the rivet diameter for beam thickness ratios of 1.0, 1.5 and 2.0, respectively, whereas the same in case of bolted joint is 3.5 times the diameter [45]. Since the zone of influence being different in both the cases, the relative spacing among the joints will be different thereby changing the magnitude of dynamic slip at the interfaces. Further, the axial load on a bolt can be varied by applying the tightening torque as per the clamping requirements of the structure whereas the preload in a rivet is constant and no control can be exercised over its magnitude. In other words, the tightening torque and initial stress are the controlling parameters in determining the axial load/preload on the bolt and rivet, respectively. Above observations suggest that the damping action in case of

both the joints are different. The motivation for the present investigation lies in developing the theory of damping mechanism in riveted structures through classical methods. The results so obtained are validated experimentally.

CHAPTER – 3

THEORETICAL ANALYSIS

3. THEORETICAL ANALYSIS:-

It is generally recognized that the damping capacity of the jointed beam and the sandwiched beam may be determined by the frictional loss energy caused by the slip at the interfaces of both steel beams and the slip between the steel beams and the sandwiched viscoelastic material. The slip found between the interfaces of jointed beam however is very small and shows very complicated characteristics, and moreover the coefficient of friction in this case may be considered smaller than the macroscopic coefficient of friction used widely in the field.

The logarithmic damping decrement, a measure of damping capacity of layered and jointed structures, is usually determined by the energy principle taking into account the relative dynamic slip and the interfacial pressure distribution at the contacting layers. The logarithmic damping decrement is evaluated theoretically for the beams with different end conditions such as; fixed-free and fixed-fixed respectively.

3.1.1 INTERFACE PRESSURE DISTRIBUTION

A layered and jointed construction is made by means of rivets that hold the members together at the interfaces. Under such circumstances, the profile of the interface pressure distribution assumes a significant role, especially in the presence of slip, to dissipate the vibration energy. Consequently, it is necessary to examine the exact nature of the interface pressure profile and its magnitude across a beam layer for the correct assessment of the damping capacity in a jointed structure. This pressure distribution at the interfaces is due to the clamping of the rivets of the contacting members.

When two or more members are pressed together by riveting, a circle of contact will be formed around the rivet with a separation taking place at a certain distance from the rivet hole as shown in Fig. 1 (a)&(b).

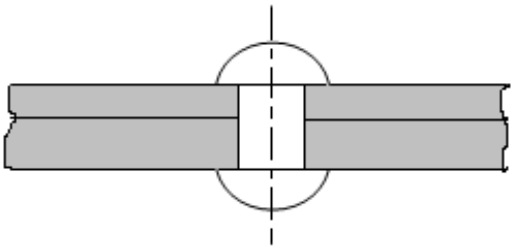

(a)

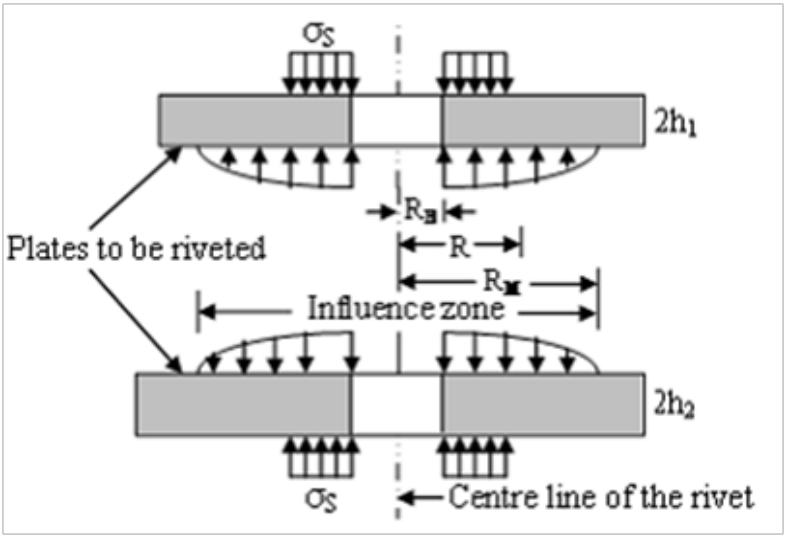

(b)

Fig. 1 (a) Plates clamped by a rivet (b) Free body diagram of a riveted joint showing the influence zone

The contact between the connecting members develops an interface pressure whose exact nature and magnitude across the beam layer is very important for the correct assessment of damping capacity of a jointed structure. As established, the contact pressure at the jointed interface is non-uniform in nature being maximum at the rivet hole and decreases with the distance away from the rivet. This allows localized slipping at the interfaces while the overall joint remains locked. Minakuchi et al. [35] have found that the interface pressure distribution due to this contact is parabolic with a circular influence zone circumscribing the rivet with diameter equal to 4.125,

5.0 and 5.6 times the diameter of the connecting rivet for thickness ratios 1.0, 1.5 and 2.0, respectively.

3.1.2 Determination of Pressure Distribution at the Interfaces

The interface pressure distribution under each rivet in a non-dimensional polynomial for layered and jointed structures is assumed as;

$$p/\sigma_S = C_1\left(R/R_B\right)^{10} + C_2\left(R/R_B\right)^{8} + C_3\left(R/R_B\right)^{6} + C_4\left(R/R_B\right)^{4} + C_5\left(R/R_B\right)^{2} + C_6 \quad (1)$$

where p, σ_S, R and R_B are the interface pressure, surface stress on the layered and jointed structure due to riveting, any radius within the influencing zone and radius of the connecting rivet, respectively and constants C_1 to C_6 of the polynomial are evaluated from the numerical data of Minakuchi et al. [35] by curve fitting using MATLAB software as shown in Table 3.1. The surface stress (σ_S) depends upon the initial tension on the rivet (P) and the area under a rivet head (A') and is evaluated from the relation $\sigma_S = P/A'$.

The distance between the rivets has been reduced inorder to achieve the uniform pressure conditions.

The above equation is an even function and a tenth order polynomial in terms of the normalized radial distance from the center of the rivet such that the function assumes its maximum value at the center of the rivet and decreases radially. It is evident from Table .1 that apart from the last two terms, values of the coefficients are relatively insignificant. This suggests for a linear profile for the pressure distribution across the interface. Damisa et al. [32] have used linear pressure profile in their analysis as an approximation. But a higher order polynomial for non-uniform interface pressure distribution has been used in the present investigation in order to obtain a good accuracy.

The distance between the rivets has been varied using the MATLAB software in order to achieve the uniform pressure condition. The final distance between the rivets to achieve the uniform pressure condition has been summarized below;

Table 1 Values of polynomial constants for different thickness ratios

THICKNESS OF PLATES	1	1.5	2
CONSTANT VALUES	c_6=0.14581228e-5 c_5=-0.57951686e-4 c_4=0.60446153e-3 c_3=0.30852824e-2 c_2=-0.95814172e-1 c_1=0.53777732	c_6=-1.737236e-7 c_5=1.398793e-5 c_4=-0.458813e-3 c_3=0.817021e-2 c_2=-0.877333e-1 c_1=0.488330	c_6=-0.7419798e-7 c_5=0.74507972e-5 c_4=-0.29801024e-3 c_3=0.62164809e-2 c_2=-0.74592085e-1 c_1=0.46039144
UNIFORM DISTANCE(R/R_B)	2.3539	2.4030	2.4340
AVERAGE PERSSURE	0.39032425	0.4055	0.4069

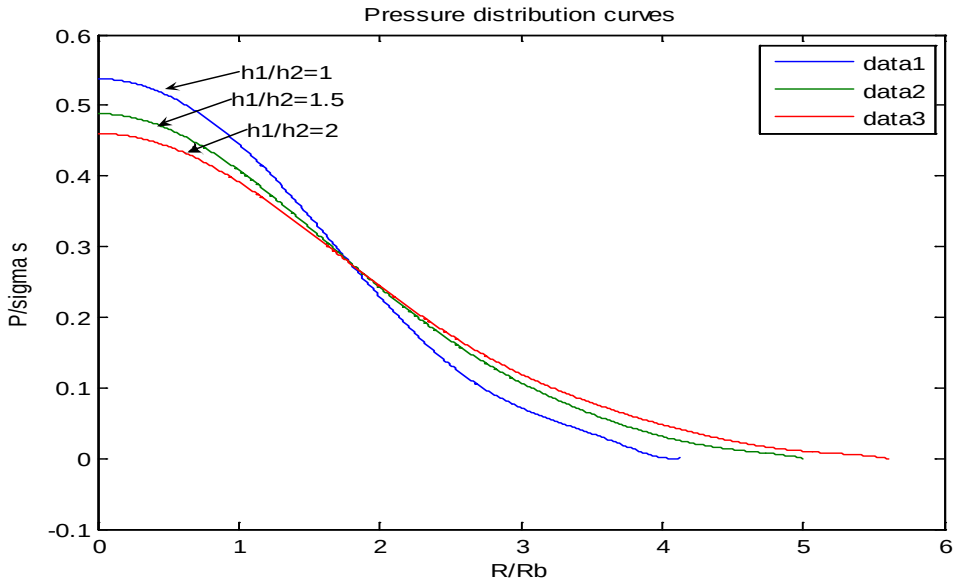

Fig. 2 Variation of Pressure distribution (P/σ_s) of different thickness of different distance(R/R_B).—Theoretical.

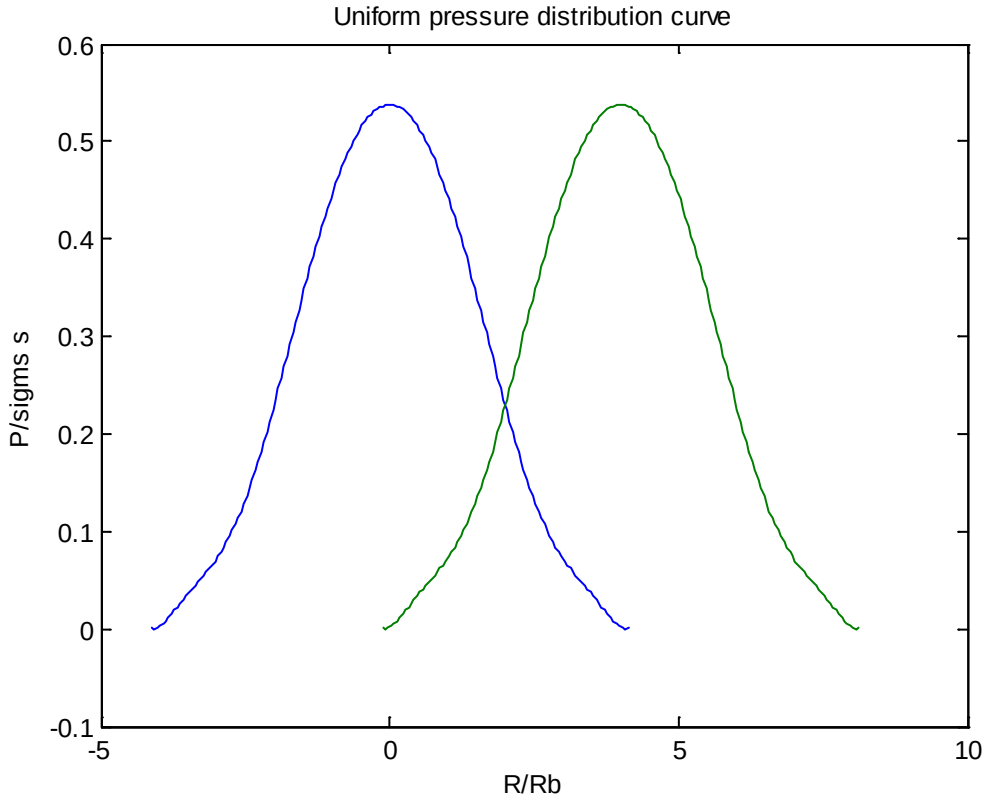

Fig. 3 Uniform pressure distribution of riveted joints

3.2 EVALUATION OF RELATIVE DYNAMIC SLIP

It is assumed that each beam of the jointed cantilever beam being vibrated has the equal bending stiffness with the same bending condition. Moreover, each layer of the beam shows no extension of the neutral axis and no deformation of the cross-section. When the jointed cantilever beam is given an initial excitation at the free end, the contacting surfaces undergo relative motion called micro-slip. This relative displacement $u(x, t)$ at any distance x from the fixed end in the absence of friction is equal to the sum of Δu_1 and Δu_2 as shown in Fig. 4 and at a particular position and time is given by Masuko et al. [15] as;

$$u(x,t) = \Delta u_1 + \Delta u_2 = 2h \tan[\partial y(x,t) / \partial x], \quad (2)$$

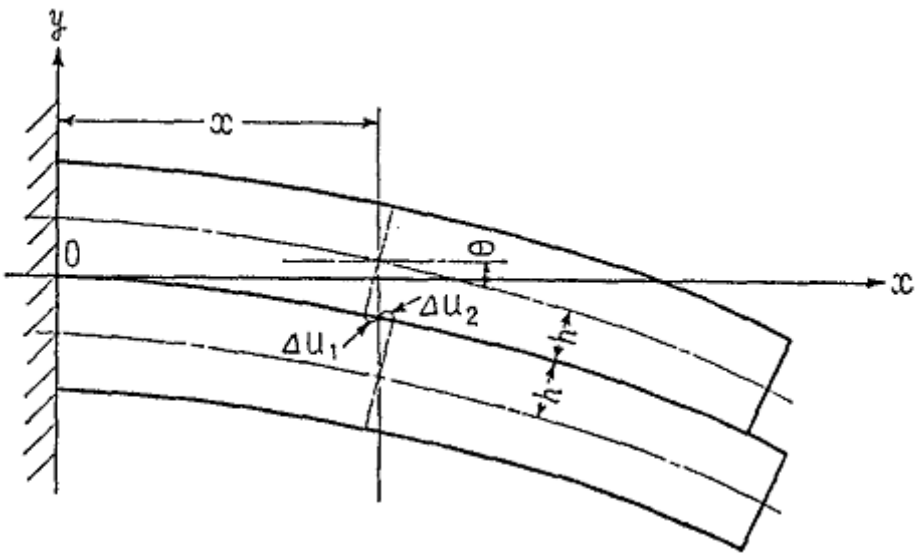

Fig. 4 Mechanism of the horizontal displacement

However, the actual relative dynamic slip [$u_r(x, t)$] at the interfaces in the presence of friction during the vibration will be less and is found out by subtracting the elastic recovery part of the relative displacement from *u(x, t)* and is rewritten as;

$$u_r(x,t) = \alpha u(x,t) = 2\alpha h \tan[\partial y(x,t) / \partial x], \quad (3)$$

where, α and $y(x,t)$ is the dynamic slip ratio and transverse deflection of the beam.

3.3 DYNAMIC EQUATIONS OF FREE TRANSVERSE VIBRATION OF CANTILEVER AND FIXED-FIXED BEAMS

3.3.1 Cantilever beam

Fig. 5 shows a cantilever beam undergoing free vibration with transverse displacement $y(x, t)$. In formulating the dynamic equations, Euler-Bernoulli beam theory is used on the assumptions that

the rotation of the differential element is negligible compared to translation and the angular distortion due to shear is small in relation to bending deformation.

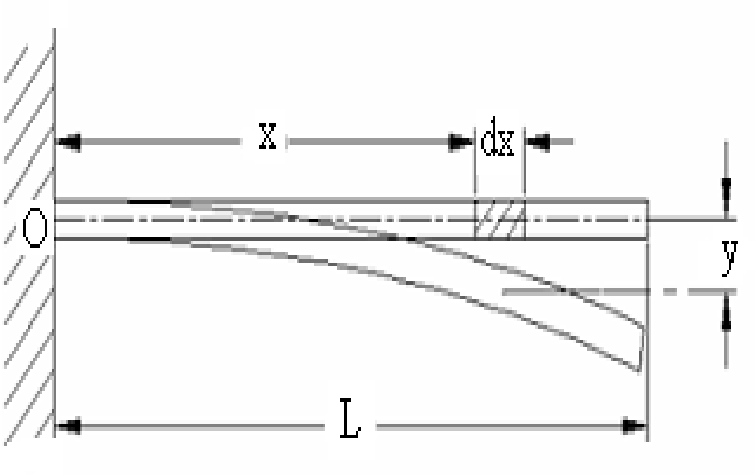

Fig. 5 Differential analysis of a beam

Vibration in cantilever beam is expressed as;

$$y(x,t) = Y(x)\, f(t) \tag{4}$$

where $Y(x)$ and $f(t)$ are the space and time function, respectively.

$f(t)$ is given by;

$$f(t) = A\cos\omega_n t + B\sin\omega_n t \tag{5}$$

where A and B are constants.

ω_n is the natural frequency.

Space function $Y(x)$ is given by;

$$Y(x) = \frac{(\cosh\lambda l - \cos\lambda l)(\sin\lambda l + \sinh\lambda l) + (\sin\lambda l - \sinh\lambda l)(\cos\lambda l + \cosh\lambda l)}{\cos\lambda l + \cosh\lambda l} \tag{6}$$

Putting equations (5) and (6) in (4) we get;

$$y(x,t) = Y(x)\left(A\cos\omega_n t + B\sin\omega_n t\right) \tag{7}$$

Putting the boundary conditions given as;

$$y(l,0) = y_0 \tag{8a}$$

$$\frac{\mathrm{d}\,y(l,0)}{\mathrm{d}\,x} = 0 \tag{8b}$$

In equation (7) and simplifying we get;

$$A = \frac{y_0}{Y(l)} \tag{9a}$$

B=0 (9b)

By inserting the values of A and B in equation (7) we get the transverse deflection of the cantilever beam at the free end as;

$$y(x,t) = Y(x)\left[\frac{y_0}{Y(l)}\cos\omega_n t\right] \tag{10}$$

3.3.2 Fixed-Fixed beam

Vibration in fixed-fixed beam is expressed as;

$$y(x,t) = Y(x)\, f(t) \tag{11}$$

where $Y(x)$ and $f(t)$ are the space and time function, respectively.

$f(t)$ is given by;

$$f(t) = A\cos\omega_n t + B\sin\omega_n t \tag{12}$$

where A and B are constants.

ω_n is the natural frequency.

Space function $Y(x)$ is given by;

$$Y(x)=\frac{(\cos\lambda l-\cosh\lambda l)(\sinh\lambda l-\sin\lambda l)+(\cosh\lambda l-\cos\lambda x)(\sinh\lambda l-\sin\lambda l)}{(\cos\lambda l-\cosh\lambda l)} \tag{13}$$

Putting equations (12) and (13) in (11) we get;

$$y(x,t)=Y(x)(A\cos\omega_n t+B\sin\omega_n t) \tag{14}$$

Putting the boundary conditions given as;

$$y\left(\frac{l}{2},0\right)=y_0 \tag{15a}$$

$$\frac{\mathrm{d}\,y\left(\frac{l}{2},0\right)}{\mathrm{d}\,x}=0 \tag{15b}$$

In equation (14) and simplifying we get;

$$A=\frac{y_0}{Y\left(\frac{l}{2}\right)} \tag{16a}$$

$$B=0 \tag{16b}$$

By inserting the values of A and B in equation (14) we get the transverse deflection of the cantilever beam at the free end as;

$$y(x,t)=Y(x)\left[\frac{y_0}{Y\left(\frac{l}{2}\right)}\cos\omega_n t\right] \tag{17}$$

3.4 ANALYSIS OF ENERGY DISSIPATED

3.4.1 Cantilever beam

Energy is dissipated due to the relative dynamic slip at the interfaces. For the above cantilever beam of length, l and height, $4h$ shown in Fig.1 (a), the interface pressure at x is expressed as $p(x)$ and the normal load acting on the length of dx is $p(x)bdx$, where b is the width of beam. Thus, the frictional force at the interfaces is given by $\mu p(x)bdx$, where μ is the coefficient of kinematic friction. By considering the condition that the interface pressure is uniformly spread over all the contact area, $p(x)$ yields p. For the above cantilever beam with uniform pressure distribution at the interfaces, p, the energy loss due to the frictional force at the interfaces per half-cycle of vibration is given by;

$$E_{loss} = \int_0^{\pi/\omega_n} \int_0^{l} \mu p b \left[\left\{ \partial u_r(x,t) / \partial t \right\} dx dt \right]. \tag{18}$$

However, the energy introduced into the layered and jointed cantilever beam in the form of strain energy per half-cycle of vibration is given by;

$$E_{ne} = \left(3EI / l^3 \right) y^2 (l, 0). \tag{19}$$

where E , $\left(I = b(4h)^3 / 12 \right)$ and $y(l,0)$ are the modulus of elasticity, cross-sectional moment of inertia and transverse deflection at the free end of the beam, respectively.

From the above equations (18) and (19), the ratio of energy is found to be;

$$\frac{E_{loss}}{E_{ne}} = \int_0^{\pi/\omega_n} \int_0^l \left[\mu pb \left\{ \partial u_r(x,t)/\partial t \right\} dxdt \right] \Big/ \left[\left(3EI/l^3 \right) y^2(l,0) \right]. \tag{20}$$

Assuming the dynamic slip ratio, α, to be independent of the distance from the fixed end of the cantilever beam and time, the above equation (20) has been modified using equation (19) as;

$$\frac{E_{loss}}{E_{ne}} = \left[2\mu bhp\alpha \Big/ \left\{ \left(3EI/l^3 \right) y^2(l,0) \right\} \right] \int_0^{\pi/\omega_n} \int_0^l \left[\partial \left\{ \tan \partial y(x,t)/\partial x \right\} dxdt \right] \Big/ \partial t \tag{21}$$

The slope of the cantilever beam $\partial y(x,t)/\partial x$ being quite small, is modified as $\tan \partial y(x,t)/\partial x \simeq \partial y(x,t)/\partial x$ .Therefore, equation (21) is re-written as;

$$\frac{E_{loss}}{E_{ne}} = \left[2\mu bhp\alpha \Big/ \left\{ \left(3EI/l^3 \right) y^2(l,0) \right\} \right] \int_0^{\pi/\omega_n} \int_0^l \left[\left\{ \partial^2 y(x,t)/\partial x \partial t \right\} dxdt \right] \tag{22}$$

By making use of the boundary and initial conditions, i.e., $y(l,0) = y_0$ and $\partial y(l,0)/\partial t = 0$, the bending deflection of beam being vibrated $y(x,t)$ can be written as;

$$y(x,t) = Y(x) \left\{ y_0 / Y(l) \right\} \cos \omega_n t, \tag{23}$$

where, *Y(x)* is the space function given by;

$$Y(x) = \left(\sinh \lambda l + \sin \lambda l \right) \left(\cosh \lambda x - \cos \lambda x \right) - \left(\cosh \lambda l + \cos \lambda l \right) \left(\sinh \lambda x - \sin \lambda x \right) \tag{24}$$

Using the above equations (21) and (22) in equation (23) and changing the limits of the time interval from 0 and π/ω_n to 0 and $\pi/2\omega_n$ and multiplying the equation by two for yielding definite solution we get;

$$E_{loss}/E_{ne} = \frac{4\mu bh\alpha}{\left(3EI/l^3\right)y^2(l,0)} \int_0^{\pi/\omega_n} \int_0^{l} \partial^2 \left[Y(x)\left\{ y_0/Y(l) \right\} \cos \omega_n t \right] dxdt \Big/ \left[\partial x/\partial t \right], \tag{25}$$

Moreover, using equations (21), (22) and (23), the energy ratio is given by;

$$E_{loss}/E_{ne} = \left[4\mu bhp\alpha\, y(l,0) \right] \Big/ \left[3\left({}^{EI}/_{l^3} \right) y^2(l,0) \right], \tag{26}$$

Replacing $3EI/l^3=k$, i.e., the static bending stiffness of the layered and riveted cantilever beam, the above equation (26) reduces to

$$E_{loss}/E_{ne} = \left[4\mu bhp\alpha \right] \Big/ \left[ky(l,0) \right]. \tag{27}$$

3.4.2 Fixed-Fixed beam

Energy is dissipated due to the relative dynamic slip at the interfaces. For the fixed-fixed beam with uniform pressure distribution at the interfaces, p, the energy loss due to the frictional force at the interfaces per half-cycle of vibration is given by;

$$E_{loss} = \int_0^{\pi/\omega_n} \int_0^{l} \mu pb \left[\left\{ \partial u_r(x,t)/\partial t \right\} dxdt \right]. \tag{28}$$

However, the energy introduced into the layered and jointed beam in the form of strain energy per half-cycle of vibration is given by;

$$E_{ne} = \left(192EI/l^3 \right) y^2 \left(\frac{l}{2}, 0 \right). \tag{29}$$

where E , $\left(I = {b(4h)^3}/{12} \right)$ and $y(l/2,0)$ are the modulus of elasticity, cross-sectional moment of inertia and transverse deflection at the midpoint of the fixed-fixed beam , respectively.

Following the above procedure for the fixed- fixed beam the energy ratio is evaluated to be;

$$E_{loss}/E_{ne} = \left[8\mu bhp\alpha y\left(\frac{l}{2},0 \right) \right] \Big/ \left[192\left({EI}/{l^3} \right) y^2\left(\frac{l}{2},0 \right) \right] \tag{30}$$

Replacing $192EI/l^3=k_f$, i.e., the static bending stiffness of the layered and riveted cantilever beam, the above equation (30) reduces to

$$E_{loss}/E_{ne} = \left[8\mu bhp\alpha \right] \Big/ \left[k_f y\left(\frac{l}{2},0 \right) \right] \tag{31}$$

where k_f is the static bending stiffness of the fixed-fixed beam.

3.5 EVALUATION OF DAMPING RATIO

The damping ratio, ψ, is expressed as the ratio of energy dissipated due to the relative dynamic slip at the interfaces and the total energy introduced into the system and is found to be;

$$\psi = \left[E_{loss} \Big/ \left(E_{loss} + E_{ne} \right) \right] = 1 \Big/ \left[1 + E_{ne}/E_{loss} \right]. \tag{32}$$

where, E_{loss} and E_{ne} are the energy loss due to interface friction and the energy introduced during the unloading process.

Putting the values of E_{loss}/E_{ne} from equations (30) and (31) in equation (32) we get the damping ratio for cantilever and fixed-fixed beam, respectively as;

$$\psi = \frac{1}{1+\left[ky(l,0)\right]/\left[4\mu bph\alpha\right]}. \tag{33}$$

$$\psi = \frac{1}{1+\left[ky\left(\frac{l}{2},0\right)\right]/\left[8\mu bph\alpha\right]}. \tag{34}$$

3.6 CALCULATION OF LOGARITHMIC DAMPING DECREMENT

Logarithmic damping decrement is used as a measure of damping capacity of a structure and is influenced by dynamic slip and interface pressure at the contacting surfaces. The logarithmic damping decrement, δ, is usually expressed as, $\delta = \ln(a_n/a_{n+1})$ where a_n is an amplitude of vibration at certain time and a_{n+1} is the amplitude of vibration after elapse of one cycle. The relationship between logarithmic damping decrement and damping ratio is written as;

$$\delta = \frac{1}{n}\ln(a_n/a_{n+1}) = \left[\ln\left\{1/(1-\psi)\right\}\right]/2$$

(35)

Putting equations (33) and (34) in (35) and simplifying, the logarithmic damping decrement for cantilever and fixed-fixed beam is given by;

$$\delta = \frac{1}{2}\ln\left[1+\frac{4\mu\alpha\, pbh}{ky(l,0)}\right] \tag{36}$$

$$\delta = \frac{1}{2}\ln\left[1+\frac{8\mu\alpha\, pbh}{ky\left(\frac{l}{2},0\right)}\right] \tag{37}$$

3.7 DETERMINATION OF THE PRODUCT OF DYNAMIC SLIP RATIO AND KINEMATICS COEFFICIENT OF FRICTION $(\alpha \times \mu)$

The accurate determination of dynamic slip ratio, α, and kinematic coefficient of friction, μ, are difficult, the product of these two parameters, i.e., $(\alpha \times \mu)$ has been found out from the experimental results for logarithmic damping decrement of 3 mm thickness beam by modifying equations (36) and (37) for the cantilever and fixed-fixed beams as;

$$\alpha \times \mu = k\left(1 - e^{-2\delta}\right) y(l, 0) \Big/ 4bphe^{-2\delta} \tag{38}$$

$$\alpha \times \mu = k_f \left(1 - e^{-2\delta}\right) y\left(l/2, 0\right) \Big/ 8bphe^{-2\delta} \tag{39}$$

The variations of $(\alpha \times \mu)$ with natural frequency of vibration at the first mode of transverse vibration have been determined under different initial amplitudes of excitation for cantilever and fixed-fixed beams and plotted as shown in Fig.6-11. These plots have been further used for evaluation of the numerical results for logarithmic damping decrement of the specimen materials with other configurations using equations (36) and (37). From the above figures it is evident that the product of coefficient of friction and slip ratio increases with the increase in the frequency and amplitude of vibration.

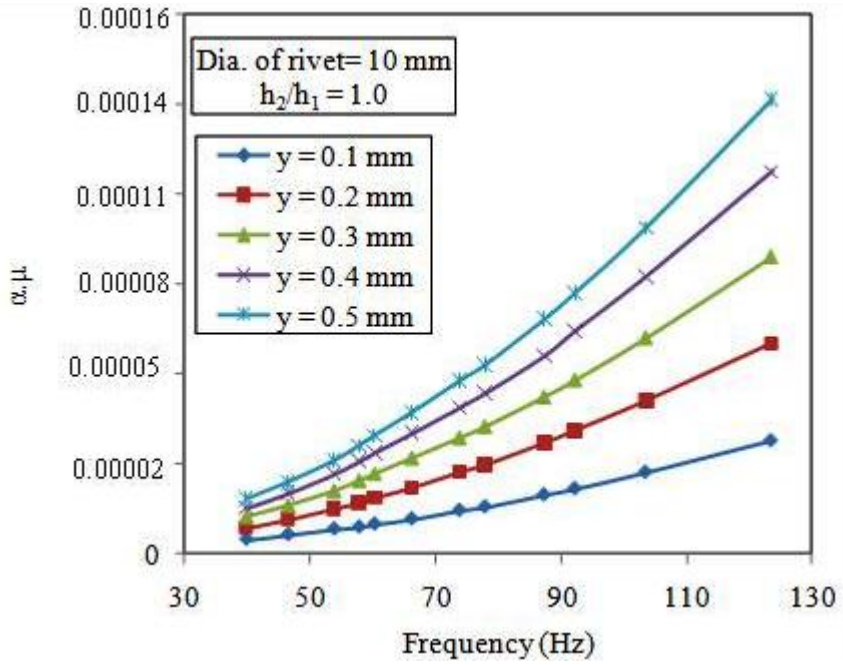

Fig. 6 Variation of $\alpha.\mu$ with frequency with beam thickness ratio 1.0 for cantilever beam at different initial amplitudes of excitation (y)

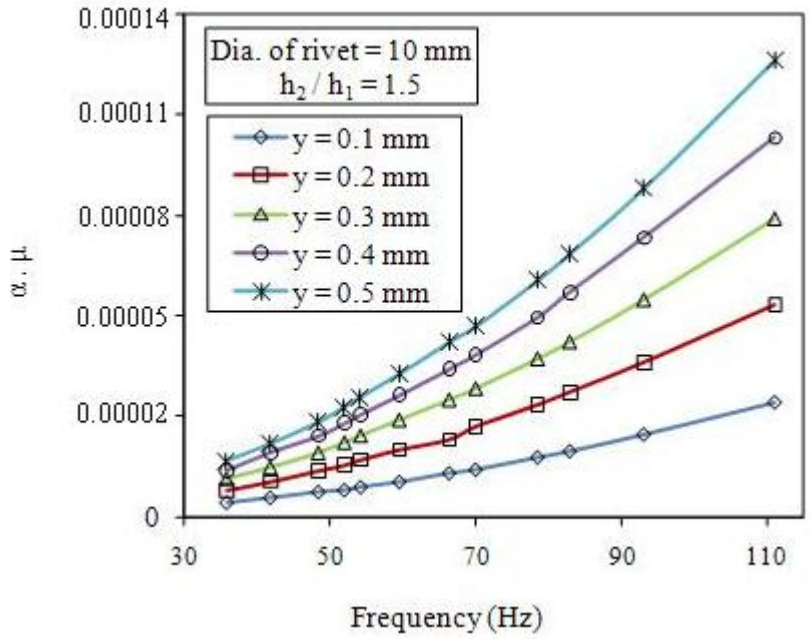

Fig. 7 Variation of $\alpha.\mu$ with frequency with beam thickness ratio 1.5 for cantilever beam at different initial amplitudes of excitation (y)

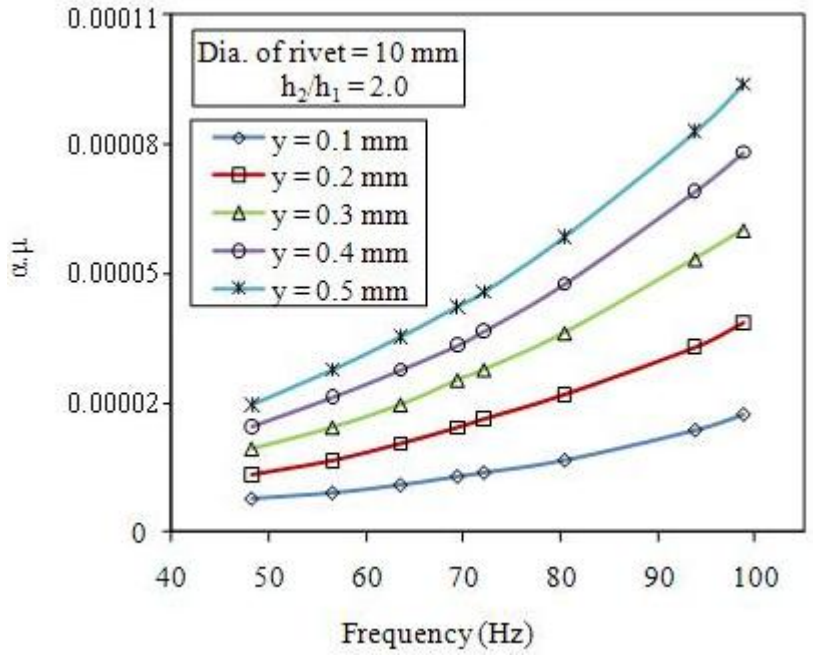

Fig. 8 Variation of $\alpha.\mu$ with frequency with beam thickness ratio 2.0 for cantilever beam at different initial amplitudes of excitation (y)

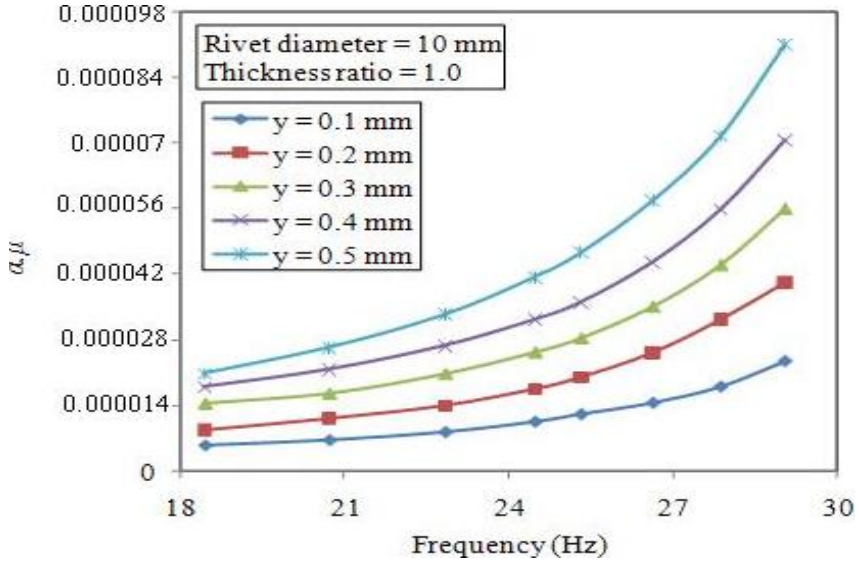

Fig. 9 Variation of $\alpha.\mu$ with frequency with beam thickness ratio 1.0 for fixed-fixed beam at different initial amplitudes of excitation (y)

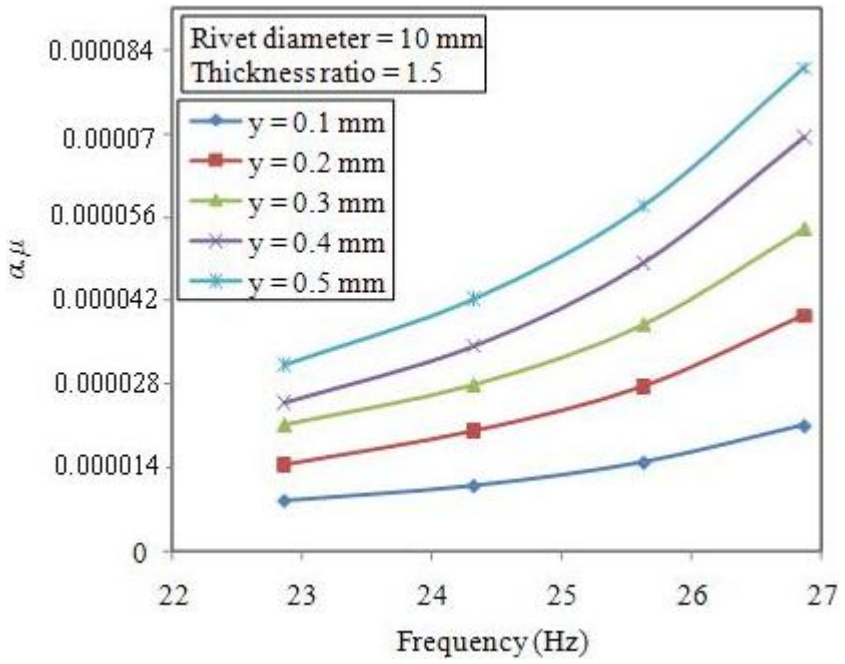

Fig. 10 Variation of $\alpha.\mu$ with frequency of vibration with beam thickness ratio 1.5 for fixed-fixed beam at different initial amplitudes of excitation (y)

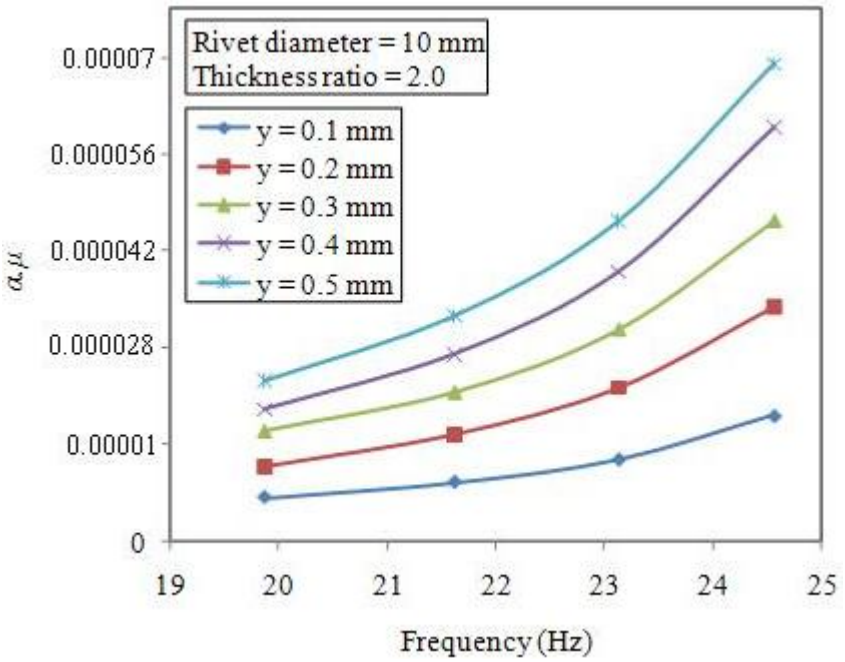

Fig. 11 Variation of $\alpha.\mu$ with frequency of vibration with beam thickness ratio 2.0 for fixed-fixed beam at different initial amplitudes of excitation (y)

CHAPTER – 4

EXPERIMENTATION

4. EXPERIMENTATION:

4.1. EXPERIMENTAL SET-UP:-

In order to evaluate the effect of different parameters on damping capacity of various types of riveted joint beams, experiments were carried out with a simple experimental set –up.

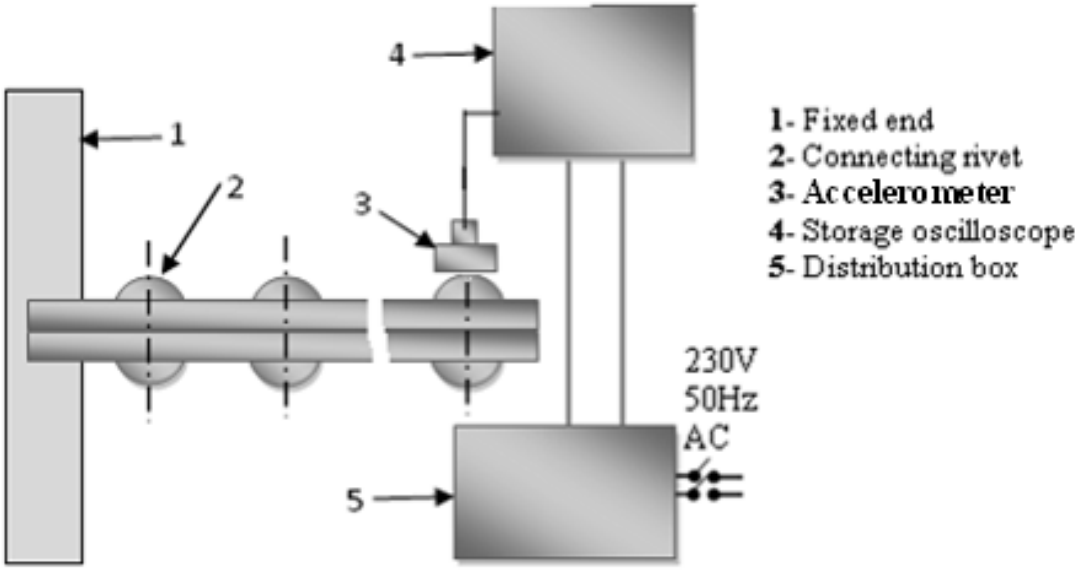

Fig. 12 Schematic diagram of experimental setup

Fig. 13 equal thickness specimen

Fig. 14 unequal thickness specimen

Fig. 15 Experiment set-up for cantilever beam (front view)

Fig. 16 Experiment set-up cantilever beam (side view)

Fig. 17 Experiment set-up for fixed-fixed beam (front view)

Fig. 18 Experiment set-up for fixed-fixed beam (side view)

4.2. TEST SPECIMEN:

Test specimens were made from mild steel from standard flats and small cutting piece of sheets. The breadth, length of specimen is kept constant and thickness of each layer is variable in multilayer but overall thickness is kept same. The types of fixing end conditions are:

(1) Fixed-Free end condition

(2) Fixed-Fixed end condition

Preparation of Specimens:-

The test specimens of different sizes are prepared from the same stock of commercial mild steel flats as presented in Tables 2 to 4 Equi-spaced rivets of 10 diameter are used to fabricate two-layered specimens with a constant clamping force. Moreover, multi-layered specimens made up of mild steel are fabricated from 10 mm diameter connecting rivets. For all these specimens, the distance between the consecutive rivets is so arranged that their influence zone just touches each other at the point of separation. The width and length of the specimens are also taken from the rivet diameter and beam thickness ratio as per the zone of influence. The length of the specimens has also been varied accordingly in order to accommodate different number of rivets. The photographs of a few specimens used in the experiments are presented in Fig. 13&14.

Table 2 Details of mild steel specimens used in the experiment for the thickness ratio 1.0

Thickness x Width (mm x mm)	Number of layers	Type of specimen	Diameter of rivet (mm)	Number of rivets used	Cantilever length (mm)
(3+3)x23.54	2	Jointed	10	10	235.4
(5+5)x23.54	2	Jointed	10	8	188.32
(6+6)x23.54	2	Jointed	10	6	141.24

Table 3 Details of mild steel specimens used in the experiment for the thickness ratio 1.5

Thickness x Width (mm x mm)	Type of specimen	Diameter of rivet (mm)	Number of rivets used	Cantilever length (mm)
(2+3)x24	Jointed	10	10	240
(4.5+3)x24	Jointed	10	8	192
(2+3)x24	Jointed	10	6	144

Table 4 Details of mild steel specimens used in the experiment for the thickness ratio 2.0

Thickness x Width (mm x mm)	Type of specimen	Diameter of rivet (mm)	Number of rivets used	Cantilever length (mm)
(3+6)x24.3	Jointed	10	10	243
(2+4)x24.3	Jointed	10	8	194.4
(2+4)x24.3	Jointed	10	6	145.8

4.3. INSTRUMENTATION:

In order to measure the logarithmic damping decrement, natural frequency of vibration of different specimen the following instruments were used as shown in circuit diagram fig:-

(1) Power supply unit

(2) Vibration pick-up

(3) Load cell

(4) Oscilloscope

(5) Dial gauge

LOAD CELL: - Specifications:-

(1) Capacity: - 5 tones

(2) Safe Over load: - 150 % of rated capacity

(3) Maximum Overload:- 200 % of rated capacity

(4) Fatigue rating: - 105 full cycles

(5) Non-linearity:- ± 1% of rated capacity or better

(6) Hysteresis: - ± 0.5 % of rated capacity or better

(7) Repeatability: - ± 0.5 % of rated capacity or better

(8) Creep error: - ± 1% of rated capacity or better

(9) Excitation: - 5 volts D.C.

(10) Terminal Resistance:-350Ω (nominal)

(11) Electrical connection: - Two meters of six core shielded cable/connected

(12) Temperature: - ± 10ċ to 50 ċ

Make: - Syscon instruments private limited, Bangalore

ENVIRONMENTAL:-

(1) Safe operating temperature: - + 10^0 C to + 50^0 C

(2) Temperature range for which specimen hold good: - + 20^0 C to + 30^0 C

OSCILLOSCOPE: -

Display: - 8x10 cm. rectangular mono-accelerator c.r.o. at 2KV e.h.t.

Vertical Deflection: - Four identical input channels ch1, ch2, ch3, ch4.

Band-width: - (-3 db) D.C. to 20 MHz (2 Hz to 20 MHz on A.C.)

Sensitivity: - 2 mV/cm to 10 V/cm in 1-2-5 sequence.

Accuracy: - ± 3 %

Variable Sensitivity :-> 2.5 % 1 range allows continuous adjustment of sensitivity from 2mV/cm to V/cm.

Input impedance: - 1M/28 PF

Input coupling: - D.C. and A.C.

Input protection: - 400 V D.C.

Display modes: - Single trace ch1 or ch2 or ch3 or ch4. Dual trace chopped or alternate modes automatically selected by the T.B. switch.

Fig. 19 Storage Oscilloscope

An oscilloscope measures two things:

- Amplitude in time domain
- Amplitude in frequency domain

An electron beam is swept across a phosphorescent screen horizontally (X direction) at a known rate (perhaps one sweep per millisecond). An input signal is used to change the position of the

beam in the Y direction. The trace left behind can be used to measure the voltage of the input signal (off the Y axis) and the duration or frequency can be read off the X axis. An oscilloscope is a test instrument which allows you to look at the 'shape' of electrical signals by displaying a graph of voltage against time on its screen. A graticule with a 1cm grid enables you to take measurements of voltage and time from the screen. The graph is the trace and is drawn by a beam of electrons striking the phosphor coating of the screen making it emit light, usually green or blue. This is similar to the way a television picture is produced. Oscilloscopes contain a vacuum tube with a cathode (negative electrode) at one end to emit electrons and an anode (positive electrode) to accelerate them so they move rapidly down the tube to the screen. This arrangement is called an electron gun. The tube also contains electrodes to deflect the electron beam up/down and left/right. The electrons are called cathode rays because they are emitted by the cathode and this gives the oscilloscope its full name of cathode ray oscilloscope or CRO.

A dual trace oscilloscope can display two traces on the screen, allowing you to easily compare the input and output of an amplifier for example. It is well worth paying the modest extra cost to have this facility.

Setting up an oscilloscope:

Oscilloscopes are complex instruments with many controls and they require some care to set up and use successfully. It is quite easy to 'lose' the trace off the screen if controls are set wrongly! There is some variation in the arrangement and labeling of the many controls so the following instructions may need to be adapted for your instrument.

1. Switch on the oscilloscope to warm up (it takes a minute or two).

2. Do not connect the input lead at this stage.

3. Set the AC/GND/DC switch (by the Y INPUT) to DC.

4. Set the SWP/X-Y switch to SWP (sweep).

5. Set Trigger Level to AUTO.

6. Set Trigger Source to INT (internal, the y input).

7. Set the Y AMPLIFIER to 5V/cm (a moderate value).

8. Set the TIMEBASE to 10ms/cm (a moderate speed).

9. Turn the time base VARIABLE control to 1 or CAL.

10. Adjust Y SHIFT (up/down) and X SHIFT (left/right) to give a trace across the middle of the screen, like the picture.

11. Adjust INTENSITY (brightness) and FOCUS to give a bright, sharp trace.

12. The oscilloscope is now ready to use!

Connecting an oscilloscope:

The Y INPUT lead to an oscilloscope should be a co-axial lead and the diagram shows its construction. The central wire carries the signal and the screen is connected to earth (0V) to shield the signal from electrical interference (usually called noise). Oscilloscopes have a BNC

socket for the y input and the lead is connected with a push and twist action, to disconnect you need to twist and pull.

An oscilloscope is connected like a voltmeter but you must be aware that the screen (black) connection of the input lead is connected to mains earth at the oscilloscope! This means it must be connected to earth or 0V on the circuit being tested.

Obtaining a clear and stable trace

Once you have connected the oscilloscope to the circuit you wish to test you will need to adjust the controls to obtain a clear and stable trace on the screen:

- The Y AMPLIFIER (VOLTS/CM) control determines the height of the trace. Choose a setting so the trace occupies at least half the screen height, but does not disappear off the screen.
- The TIMEBASE (TIME/CM) control determines the rate at which the dot sweeps across the screen. Choose a setting so the trace shows at least one cycle of the signal across the screen. Note that a steady DC input signal gives a horizontal line trace for which the time base setting is not critical.
- The TRIGGER control is usually best left set to AUTO.

  Measuring voltage and time period:

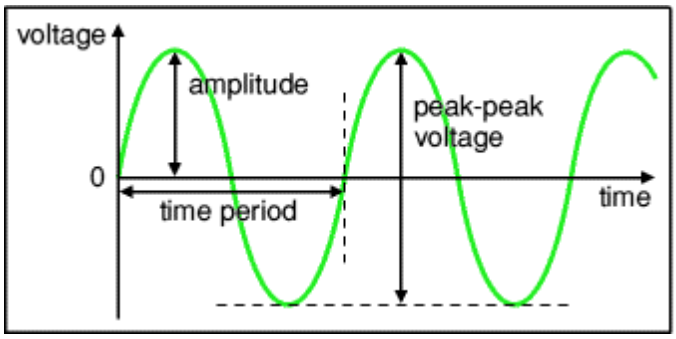

Fig. 20 Relation between voltage and time

The trace on an oscilloscope screen is a graph of voltage against time. The shape of this graph is determined by the nature of the input signal.

In addition to the properties labeled on the graph, there is frequency which is the number of cycles per second. The diagram shows a sine wave but these properties apply to any signal with a constant shape.

- Amplitude is the maximum voltage reached by the signal. It is measured in volts, V.
- Peak voltage is another name for amplitude.
- Peak-peak voltage is twice the peak voltage (amplitude). When reading an oscilloscope trace it is usual to measure peak-peak voltage.
- Time period is the time taken for the signal to complete one cycle. It is measured in seconds (s), but time periods tend to be short so milliseconds (ms) and microseconds (μs) are often used. 1ms = 0.001s and 1μs = 0.000001s.
- Frequency is the number of cycles per second. It is measured in hertz (Hz), but frequencies tend to be high so kilohertz (kHz) and megahertz (MHz) are often used. 1kHz = 1000Hz and 1MHz = 1000000Hz.

Voltage:

Voltage is shown on the vertical y-axis and the scale is determined by the Y AMPLIFIER (VOLTS/CM) control. Usually peak-peak voltage is measured because it can be read correctly even if the position of 0V is not known. The amplitude is half the peak-peak voltage. To read the amplitude voltage directly you must check the position of 0V (normally halfway up the screen): move the AC/GND/DC switch to GND (0V) and use Y-SHIFT (up/down) to adjust the position of the trace if necessary, switch back to DC afterwards so you can see the signal again. Voltage = distance in cm × volts/cm.

Time period:

Time is shown on the horizontal x-axis and the scale is determined by the TIMEBASE (TIME/CM) control. The time period (often just called period) is the time for one cycle of the signal. The frequency is the number of cycles per second, frequency = 1/time period Ensure that the variable time base control is set to 1 or CAL (calibrated) before attempting to take a time reading.

Dial indicator:

Dial indicator are instruments used to accurately measure a small distance. They may also be known as a dial gauge, Dial test indicator (DTI), or as a “clock”. They are named so because the measurement results are displayed in a magnified way by means of a dial. Dial indicator may be used to check the variation in tolerance during the inspection process of a machined part, measure the deflection of a beam or ring under laboratory conditions, as well as many other situations where a small measurement needs to be registered or indicated.

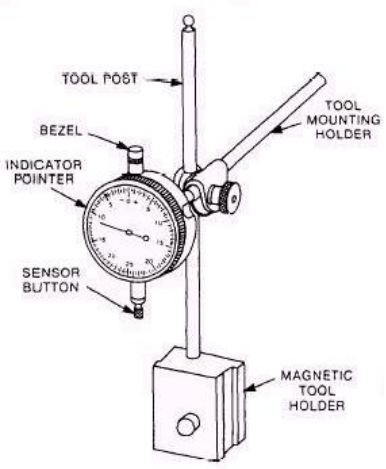

Fig. 21 Dial indicator

Vibration pick-up:-

Type: - MV-2000. Specifications:-

(1) Dynamic frequency range: - 2 c/s to 1000 c/s

(2) Vibration amplitude: - ±1.5 mm max.

(3) Coil resistance: - 1000Ω

(4) Operating temperature: - 10ċ to 40 ċ

(5) Mounting: - by magnet

(6) Dimensions: - cylindrical Length:-45 mm Diameter: - 19 mm

(7) Weight: - 150 grams

Fig. 22 vibration pick-up

Velocity Transducer:

The velocity pickup is a very popular transducer or sensor for monitoring the vibration of rotating machinery. This type of vibration transducer installs easily on machines, and generally costs less than other sensors. For these two reasons, this type of transducer is ideal for general purpose machine applications. Velocity pickups have been used as vibration transducers on rotating machines for a very long time, and they are still utilized for a variety of applications today. Velocity pickups are available in many different physical configurations and output sensitivities.

Theory of Operation

When a coil of wire is moved through a magnetic field, a voltage is induced across the end wires of the coil. The induced voltage is caused by the transferring of energy from the flux field of the

magnet to the wire coil. As the coil is forced through the magnetic field by vibratory motion, a voltage signal representing the vibration is produced.

Signal Conventions

A velocity signal produced by vibratory motion is normally sinusoidal in nature. In other words, in one cycle of vibration, the signal reaches a maximum value twice in one cycle. The second maximum value is equal in magnitude to the first maximum value, but opposite in direction. By definition velocity can be measured in only one direction. Therefore, velocity measurements are typically expressed in zero to peak, RMS units. RMS units may be specified on permanent monitor installations to allow correlation with information gathered from portable data collectors.

Another convention to consider is that motion towards the bottom of a velocity transducer will generate a positive going output signal. In other words, if the transducer is held in its sensitive axis and the base is tapped, the output signal will go positive when it is initially tapped.

Construction

The velocity pickup is a self-generating sensor requiring no external devices to produce a vibration signal. This type of sensor is made of three components: a permanent magnet, a coil of wire, and spring supports for the coil of wire. The pickup is filled with an oil to dampen the spring action. Due to gravity forces, velocity transducers are manufactured differently for horizontal or vertical axis mounting. With this in mind, the velocity sensor will have a sensitive axis that must be considered when applying these sensors to rotating machinery. Velocity sensors are also susceptible to cross axis vibration, which if great enough may damage a velocity sensor.

Wire is wound onto a hollow bobbin to form the wire coil. Sometimes, the wire coil is counter wound (wound one direction and then in the opposite direction) to counteract external electrical fields. The bobbin is supported by thin, flat springs to position it accurately in the permanent magnet's field

4.4. EXPERIMENTAL TECHNIQUES:-

In order to compare the numerical results evaluated by the theory with the actual logarithmic damping decrement of layered and riveted jointed beams, a series of experiments were conducted. The experimental set-up for cantilever and fixed-fixed beams with detailed instrumentation is shown in Fig. 15-18. All specimens were tested for their natural frequency, amplitudes and logarithmic damping decrement. A load cell was placed on the ground and above it a packing was given on which the specimen is kept. Above the plate a screwed spindle is mounted by rotating the screw clockwise, load is applied on the specimen as well as load cell. A certain load as per experiment is applied at the fixed end of each of the specimens. The free end and midpoint of cantilever and fixed-fixed beams, respectively of the specimens was excited with a spring. The excitation amplitude given to the specimen is indicated in the dial gauge. Vibration signal was picked up with the help of vibration pick-up and it was fed to oscilloscope. From there it is fed to oscilloscope where amplitude and frequency of the test signal were measured. From this logarithmic damping decrement and frequency of vibration were measured. The specimens were prepared from commercial mild steel strips as shown in Tables 1-3, by joining two or more layers using riveted joints. The lengths of the specimens were varied, the specimens are rigidly fixed to the support to obtain perfect end conditions and the first experiments were conducted to determine the bending modulus of elasticity (E) of the specimen

materials. Solid specimens made from the same stock of commercial mild steel strips were held rigidly at the fixed end and their deflection (Δ) was measured by applying different static loads W. From these static loads and the corresponding deflections, the average static bending stiffness (W/Δ) was determined. The bending modulus for the specimen material was then evaluated using the equation $E = \left(\frac{W}{\Delta}\right)\left(\frac{l^3}{3I}\right)$. The static bending stiffness (k) of the jointed specimens was determined and found to be always lower than that of an equivalent solid specimen. The logarithmic damping decrement and natural frequency of vibration of all the specimens were determined experimentally at their first mode of free vibration. The lengths of these specimens were also varied during experimentation. A spring loaded exciter was used to excite the specimens. Tests were conducted using various amplitudes of excitation (0.1, 0.2, 0.3, 0.4, 0.5 mm.) for all the specimens tested under the different conditions. The free vibration was sensed with a magnet based vibration pick-up and the corresponding signal was fed to a storage oscilloscope to obtain a steady signal. The logarithmic damping decrement was then evaluated from the measured values of the amplitudes of the first cycle (a_1), last cycle (a_{n+1}) and the number of cycles (n) of the steady signal by using the equation; $\delta = \frac{1}{n}\ln\left(\frac{a_1}{a_{n+1}}\right)$. The corresponding natural frequency and time period for the first mode of vibration of the layered and jointed beam is directly recorded from the storage oscilloscope.

CHAPTER – 5

RESULTS AND DISCUSSION

5.1.RESULTS:

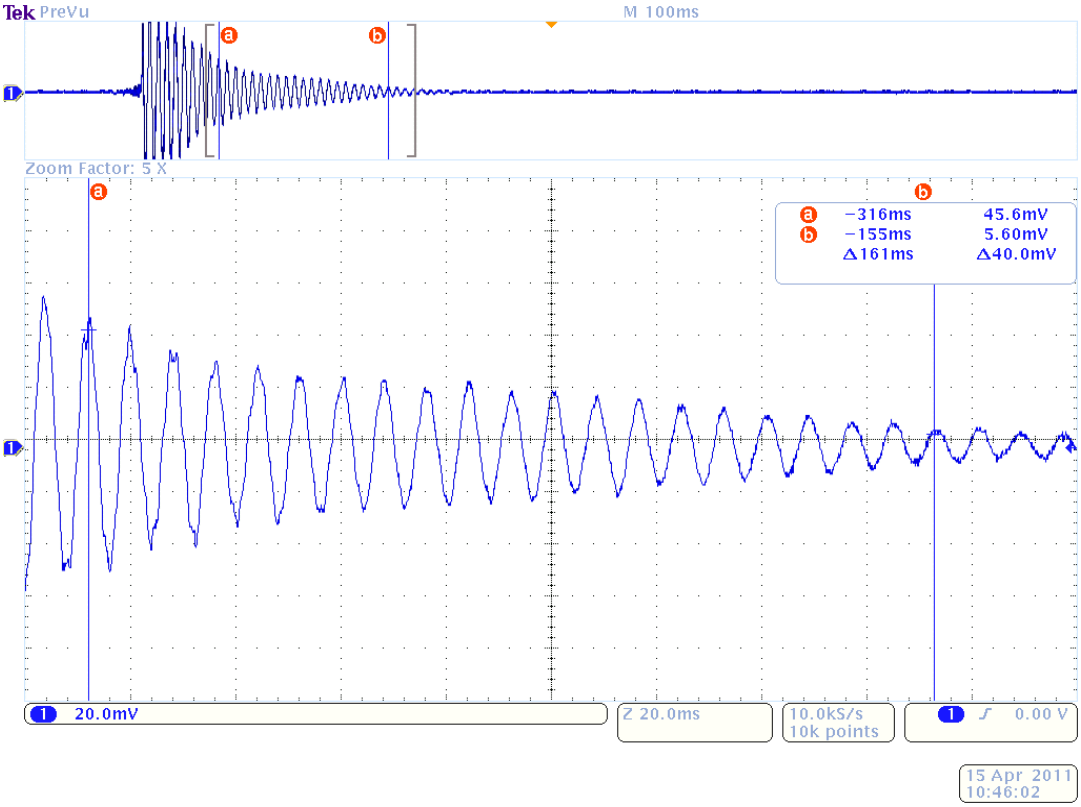

Fig. 23 photograph of result of experiment by oscilloscope for cantilever beam

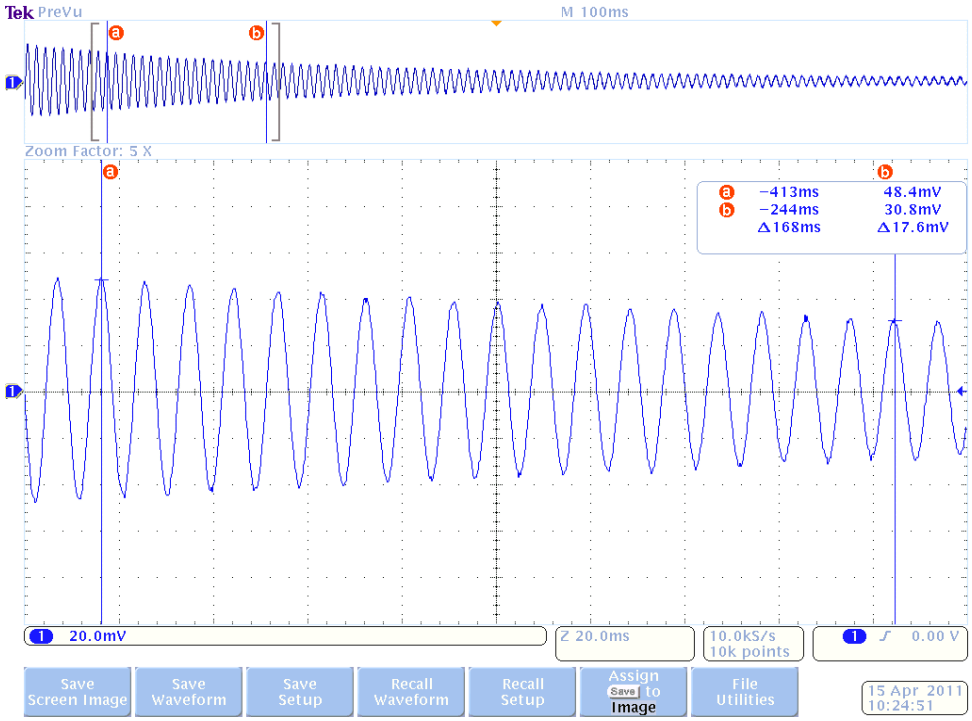

Fig. 24 photograph of result of experiment by oscilloscope for fixed-fixed beam.

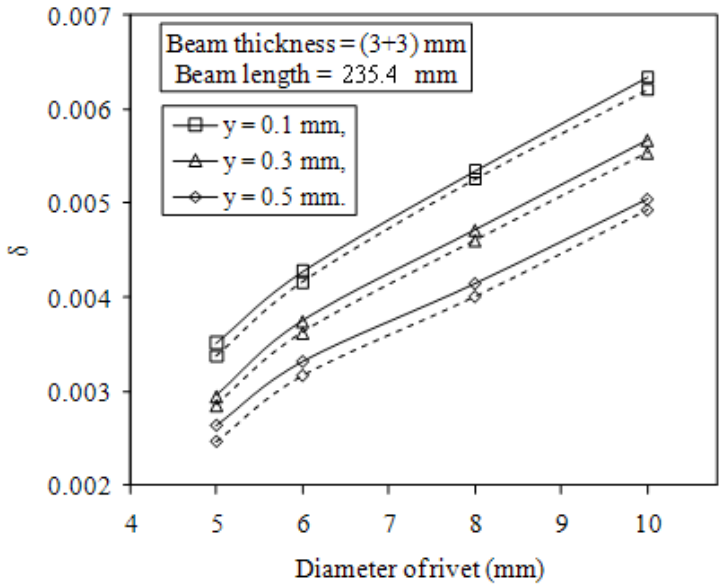

Fig. 25 Variation of logarithmic decrement with the diameter of rivet for mild steel specimens of cantilever with beam length 235.4 mm and thickness (3+3) mm at different amplitudes of excitation (y).

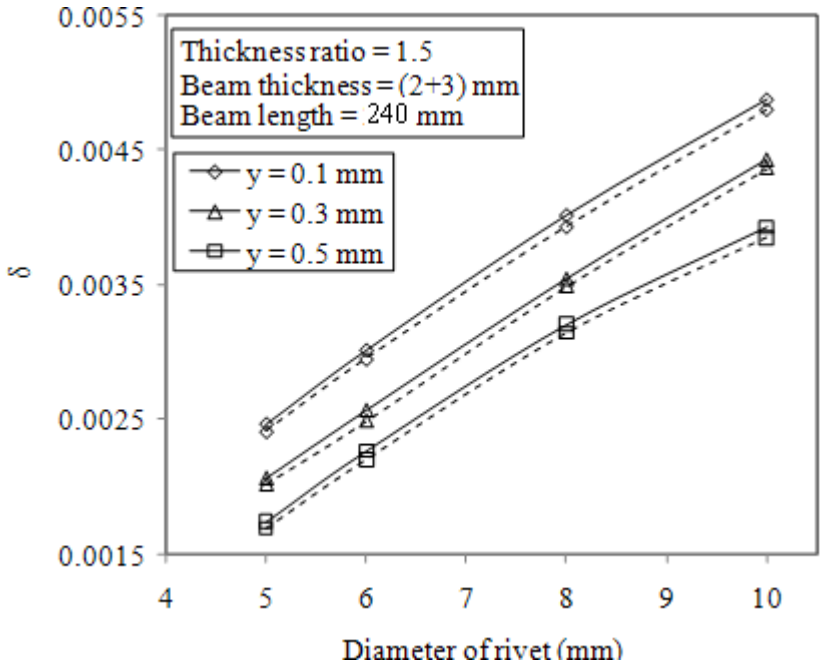

Fig. 26 Variation of logarithmic decrement with the diameter of rivet with beam length 240 mm and thickness (2+3) mm at different amplitudes of excitation (y)

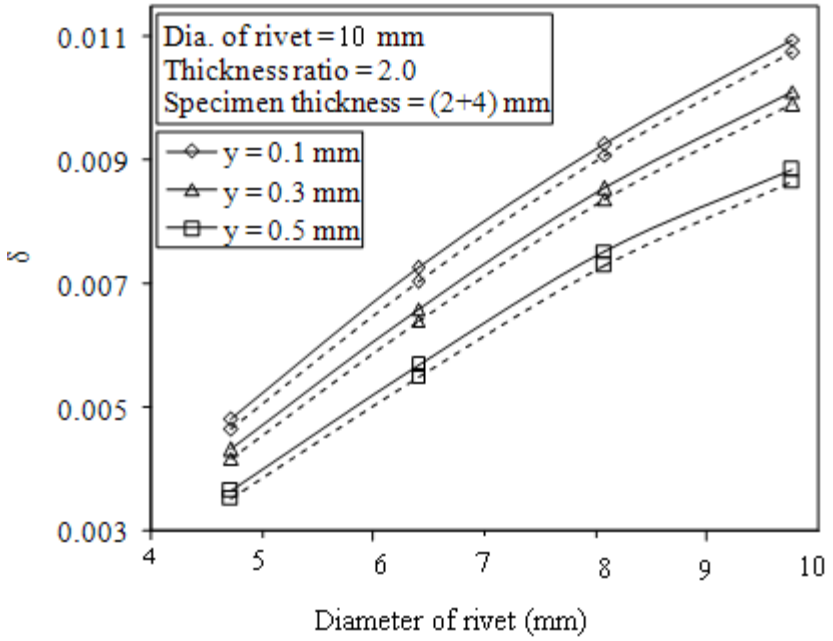

Fig. 27 Variation of logarithmic decrement with the diameter of rivet with beam length 243 mm and thickness (2+4) mm at different amplitudes of excitation (y)

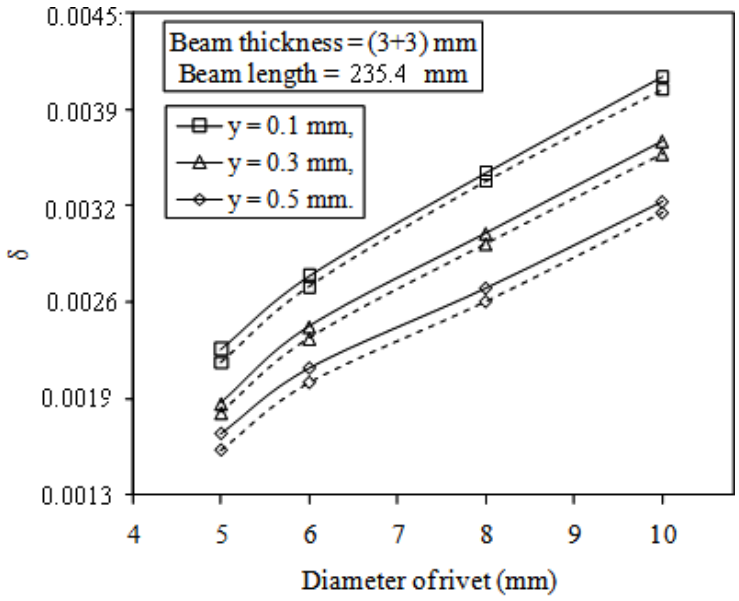

Fig. 28 Variation of logarithmic decrement with the diameter of rivet for mild steel specimens of fixed-fixed with beam length 235.4 mm and thickness (3+3) mm at different amplitudes of excitation (y)

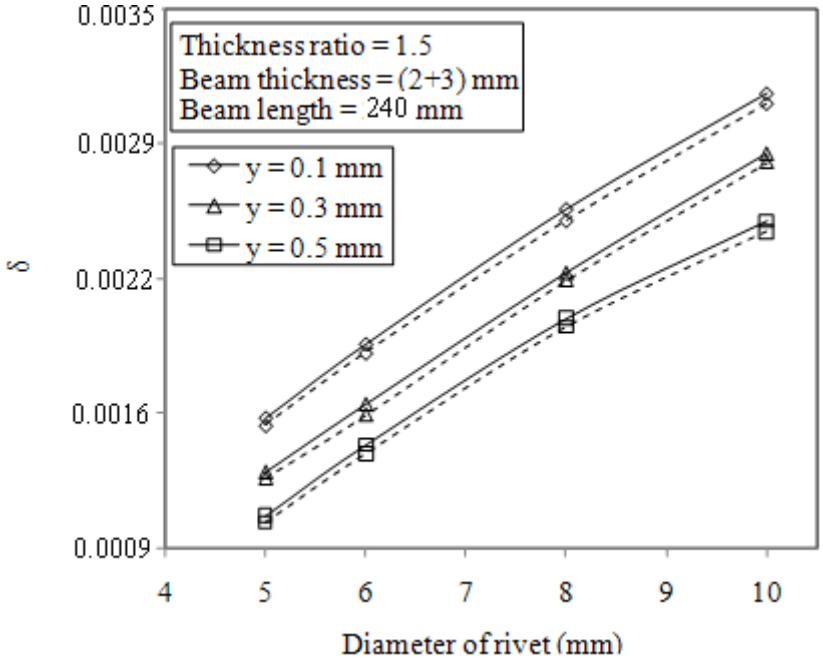

Fig. 29 Variation of logarithmic decrement with the diameter of rivet with fixed-fixed beam length 240 mm and thickness (2+3) mm at different amplitudes of excitation (y)

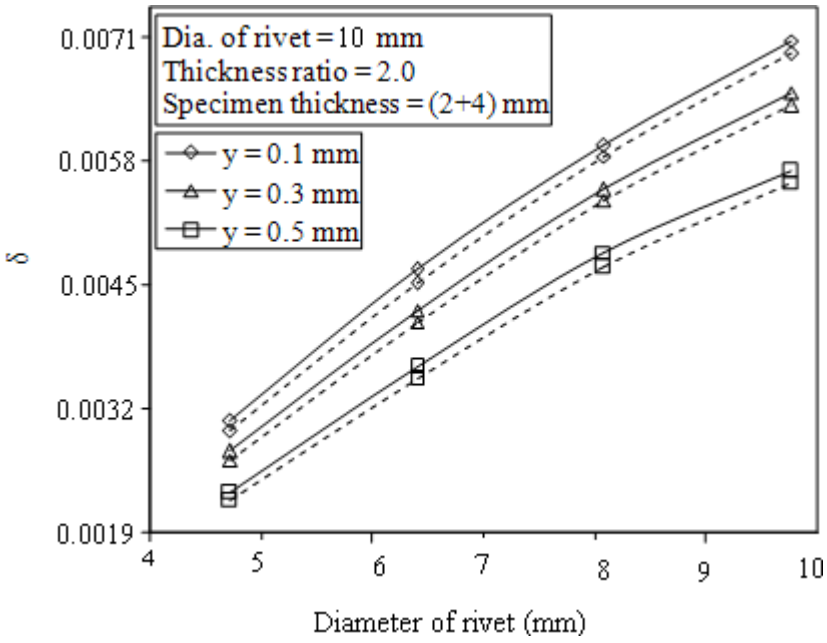

Fig. 30 Variation of logarithmic decrement with the diameter of rivet with fixed-fixed beam length 243 mm and thickness (2+4) mm at different amplitudes of excitation (y)

5.2. DISCUSSION

From the experimental results, the following salient points have been observed and discussed in details as given below.

(1) Damping ratio of layered and jointed structures decreases with increase in the initial amplitude of excitation. With an increase in initial amplitude of excitation the input strain energy into the system is increased. Also with the increase in initial amplitude of excitation the energy loss also increses.However, the rate of loss of energy is less compared to input strain energy thereby resulting in lower damping.

(2) Damping ratio of layered and jointed structures increases with decreases the distance between riveted joints and maintain uniformity throughout the contacting surface for a particular spacing of the connecting rivets which has been found to be 2,3539 times the diameter of the rivet.

(3) Damping ratio of layered and jointed structures increases with an increase in the length. The increase in length results in an increased interface length thereby resulting in an increased area for energy dissipation of the structures. Thus increased contact area results in more energy dissipation.

CHAPTER – 6

CONCLUSION AND SCOPE FOR FURTHER WORK

6.1. CONCLUSION

Mechanical joints and fasteners are primary sources of improving damping in structural design caused by friction and micro-slip between the interfaces. The damping of jointed riveted structures has been studied theoretically considering the energy loss due to friction and the dynamic slip at the contacting layers. Further, the theoretical results obtained by using mathematical models have been verified by conducting extensive experiments for the validation of results. From the foregoing discussions, it is found that the damping of layered and riveted structures can be improved by the following influencing parameters: (a) amplitude of excitation, (b) frequency of excitation, (c) length of specimens (d) end condition of the beam specimen. Finally, it is established that a useful increase in the inherent damping in a jointed structure can be achieved at lower initial excitation, greater number of layers and larger length of specimens. The riveted structures being largely used in bridges, pressure vessels, frames, trusses and machine members can be effectively designed to enhance the damping characteristics so as to minimize the disastrous effects of vibration and thereby increasing their life.

6.2. SCOPE OF FURTHER WORK

1. Study of damping may be studied for riveted structures consisting of layers of different materials

2. The present analysis has been developed for beam-like structures; it may be studied for flat plates.

3. Damping of riveted structures can be studied in the vacuum condition for the correct evaluation of damping.

4. Present analysis can be extended for forced vibration conditions.

REFERENCES

1. Cochardt, A.W., 1954, A method for determining the internal damping of machine members, ASME, Journal of Applied Mechanics, Vol. 76, No. 9, pp. 257-262.

2. Goodman, L.E. and Klumpp, J.H., 1956, Analysis of slip damping with reference to turbine-blade vibration, ASME, Journal of Applied Mechanics, Vol. 23, pp. 421–429.

3. Beards, C.F., 1992, Damping in structural joints, The Shock and Vibration Digest, Vol. 24, No. 7, pp. 3-7.

4. Ungar, E.E., 1973, The status of engineering knowledge concerning the damping of built-up structures, Journal of Sound and Vibration, Vol. 26, No. 1, pp. 141-154.

5. Gaul, L. and Nitsche, R., 2001, The role of friction in mechanical joints, ASME, Applied Mechanics Reviews, Vol. 54, No. 2, pp. 93-106.

6. Hartwigsen, C.J., Song, Y., Mcfarland, D.M., Bergman, L.A. and Vakakis, A.F., 2004, Experimental study of non-linear effects in a typical shear lap joint configuration, Journal of Sound and Vibration, Vol. 277, No. 1-2, pp. 327-35.

7. Pratt, J.D. and Pardoen, G., 2002, Numerical modeling of bolted lap joint behavior, Journal of Aerospace Engineering, Vol. 15, No. 1, pp. 20-31.

8. Beards, C.F. and Imam, I.M.A., 1978, The damping of plate vibration by interfacial slip between layers, International Journal of Machine Tool Design and Research, Vol. 18, No. 3, pp. 131-137.

9. Beards, C.F. and Williams, J.L., 1977, The damping of structural vibration by rotational slip in joints, Journal of Sound and Vibration, Vo1. 53, No. 3, pp. 333-340.

10. Beards, C.F. 1975, Some effects of interface preparation on frictional damping in joints, International Journal Machine Tool Design and Research, Vol. 15, No. 1, pp. 77-83.

11. Menq, C.-H., Bielak, J. and Griffin, J.H., 1986, The influence of microslip on vibratory response, Part I: A new microslip model, Journal of Sound and Vibration, Vol. 107, No. 2, pp. 279-293.

12. Menq, C.H., Griffin, J.H. and Bielak J., 1986, The influence of microslip on vibratory response, Part II: A comparison with experimental results, Journal of Sound and Vibration, Vol. 107, No. 2, pp. 295-307.

13. Hansen, S.W. and Spies, R.D., 1997, Structural damping in laminated beams due to interfacial slip, Journal of Sound and Vibration, Vol. 204, No. 2, pp. 183-202.

14. Masuko, M., Ito, Y. and Yoshida, K., 1973, Theoretical analysis for a damping ratio of a jointed cantibeam, Bulletin of JSME, Vol. 16, No. 99, pp. 1421-1432.

15. Nishiwaki, N., Masuko, M., Ito, Y. and Okumura, I., 1978, A study on damping capacity of a jointed cantilever beam, 1st Report: Experimental results, Bulletin of JSME, Vol. 21, No. 153, pp. 524-531.

16. Nishiwaki, N., Masuko, M., Ito, Y. and Okumura, I., 1980, A study on damping capacity of a jointed cantilever beam, 2nd Report: Comparison between theoretical and experimental values, Bulletin of JSME, Vol. 23, No. 177, pp. 469-475.

17. Olofsson, U. and Hagman, L., 1997, A model for micro-slip between flat surfaces based on deformation of ellipsoidal elastic bodies, Tribology International, Vol. 30, No. 8, pp. 599-603.

18. Thomson, W.T., 1993, Theory of Vibration with Applications, 2nd Edition, George Allen and Unwin, London.

19. Den Hartog, J.P., 1931, Forced vibrations with combined coulomb and viscous friction, Transactions of the ASME, Vol. 53, No. 9, pp. 107-115.

20. Gaul, L. and Nitsche, R., 2000, Friction control for vibration suppression, Mechanical Systems and Signal Processing, Vol. 14, No. 2, pp. 139-150.

21. Clarence W. de Silva, 2000, Vibration: Fundamentals and Practice, CRC Press LLC, Boca Raton.

22. Sidorov, O.T., 1983, Change of the damping of vibrations in the course of operation in dependence on the parameters of bolted joints, Strength of Materials, Vol. 14, pp. 671–674.

23. El-Zahry, R.M., 1985, Investigation of the vibration behavior of pre-loaded bolted joints, Dirasat-Engineering Technology, Vol. 12, pp. 201–223.

24. Marshall, M.B., Lewis, R. and Dwyer-Joyce, R.S., 2006, Characterization of contact pressure distribution in bolted joints, Strain, Vol. 42, No. 1, pp. 31-43.

25. Kaboyashi, T. and Matsubayashi, T., 1986, Consideration on the improvement of the stiffness of bolted joints in machine tools, Bulletin of JSME, Vol. 29, pp. 3934–3937.

26. Tsai, J.S. and Chou, Y.F., 1988, Modelling of dynamic characteristics of two-bolted joints, Journal of Chinese Institute of Engineering, Vol. 11, pp. 235–245.

27. Shin, Y.S., Iverson, J.C. and Kim, K.S., 1991, Experimental studies on damping characteristics of bolted joints for plates and shells, ASME, Journal of Pressure Vessel Technology, Vol. 113, No. 3, pp. 402–408.

28. Gould, H.H. and Mikic, B.B., 1972, Areas of contact and pressure distribution in bolted joints, ASME, Journal of Engineering for Industry, Vol. 94, No. 3, pp. 864–870.

29. Ziada, H.H. and Abd, A.K., 1980, Load pressure distribution and contact areas in bolted joints, Institute of Engineers (India), Vol. 61, pp. 93–100.

30. Nanda, B.K. and Behera, A.K., 1999, Study of damping in layered and jointed structures with uniform pressure distribution at the interfaces, Journal of Sound and Vibration, Vol. 226, No. 4, pp.607-624.

31. Damisa, O., Olunloyo, V.O.S., Osheku, C.A. and Oyediran, A.A., 2007, Static analysis of slip damping with clamped laminated beams, European Journal of Scientific Research, Vol. 17, No. 4, pp. 455-476.

32. Damisa, O., Olunloyo, V.O.S., Osheku, C.A. and Oyediran, A.A., 2008, Dynamic analysis of slip damping in clamped layered beams with non-uniform pressure distribution at the interface, Journal of Sound and Vibration, Vol. 309, No. 3-5, pp. 349-374.

33. Olunloyo, V.O.S., Damisa, O., Osheku, C.A. and Oyediran, A.A. 2007, Further results on static analysis of slip damping with clamped laminated beams, European Journal of Scientific Research, Vol. 17, No. 4, pp. 491-508.

34. Minakuchi, Y., Yoshimine, K., Koizumi, T. and Hagiwara, T., 1985, Contact pressure measurement by means of ultrasonic waves: On a method of quantitative measurement, Bulletin of JSME, Vol. 28, No. 235, pp. 40-45.

35. Minakuchi, Y., 1985, Contact pressure measurement by means of ultrasonic waves: On a bolted joint with a solid-metal flat gasket, Bulletin of JSME, Vol. 28, No. 239, pp. 792-798.

36. Minakuchi, Y., Koizumi, T. and Shibuya, T., 1985, Contact pressure measurement by means of ultrasonic waves using angle probes, Bulletin of JSME, Vol. 28, No. 243, pp. 1859-1863.

37. Hanks, B.R. and Stephens, D.G., 1967, Mechanisms and scaling of damping in a practical structural joint, Shock and Vibration Bulletin, Vol. 36, pp. 1–8.

38. Brown, C.B., 1968, Factors affecting the damping in a lap joint, ASCE, Journal of Structural Division, Vol. 94, pp. 1197–1217.

39. Beards, C.F., 1983, The damping of structural vibration by controlled interface slip in joints, ASME, Journal of Vibration, Acoustics, Stress and Reliability and in Design, Vol. 105, No. 3, pp. 369–373.

40. Jezequel, L., 1983, Structural damping by slip in joints, ASME, Journal of Vibration, Acoustics Stress, Reliability and Design, Vol. 105, No. 2, pp. 497–504.

41. Padmanabhan, K.K. and Murty, A.S.R., 1991, Damping in structural joints subjected to tangential loads, Journal of the Structural Division, Proceedings of Institute of mechanical Engineers, Vol. 205, pp. 121–129.

42. Beards, C.F. and Woodwat, A., 1985, The control of frame vibration by friction damping in joints, ASME, Journal of Vibration, Acoustics, Stress Analysis, Reliability and Design, Vol. 107, pp. 27–32.

43. Pian, T.H.H. and Hallowell, F.C., 1950, Investigation of structural damping in simple built-up beams, Technical Report, Aeroelastic and Structures Laboratory, Massachusetts Institute of Technology, Cambridge, Mass.

44. Pian, T.H.H., 1957, Structural damping of a simple built-up beam with riveted joints in bending, ASME, Journal of Applied Mechanics, Vol. 24, pp. 35–38.

45. Nanda, B.K., 2006, Study of the effect of bolt diameter and washer on damping in layered and jointed structures, Journal of Sound and Vibration, Vol. 290, No. 3-5, pp. 1290-1314.